Numerical investigation of the superfluid transition in low dimensions and in anisotropic systems

by

Phong Hai Nguyen

A thesis submitted in partial fulfillment of the requirements for the degree of

Master of Science

Department of Physics
University of Alberta

Abstract

The main theme of this thesis is the superfluid transition in reduced dimensions and in anisotropic and inhomogeneous systems. Using state-of-the-art computational methodology, we carry out large-scale, numerically exact computer simulations to study this topic, making use of classical and quantum lattice models. In particular, we investigate the behavior of the specific heat in two-dimensional (2D) superfluids, using the classical x-y Hamiltonian on the square lattice as a minimal, paradigmatic model. The specific heat is found to exhibit a well-defined peak in the thermodynamic limit, at a temperature above the superfluid transition temperature. We then attempt to explore a possible dimensional crossover in a 2D superfluid in the presence of an externally imposed density modulation, in the context of the $|\psi|^4$ classical field theory. As the strength of the modulation increases, the physics of the system becomes more similar to that of the anisotropic $x - y$ model, characterized by a decreased superfluid transition temperature and an anisotropic response, but with no dimensional crossover. Finally, we examine the phase diagram of lattice hard core bosons with anisotropic nearest-neighbor interactions that can vary between repulsion and attraction in different directions. This phase diagram includes a superfluid phase, as well as two crystalline phases at half-filling, either checkerboard or striped, but no "supersolid" phase; which is similar to the case of isotropic interactions. Our predictions appear to be in principle testable experimentally, for example by performing measurements on thin films of superfluid helium or cold atom assemblies.

Preface

The entirety of this thesis constitutes the original thesis research of Phong Hai Nguyen, under the supervision of Professor Massimo Boninsegni.

Chapter 3 of this work has been published as Phong H. Nguyen and Massimo Boninsegni, "Superfluid transition and specific heat of the 2D x-y model: Monte Carlo simulation", Applied Sciences **11**, 4931 (2021).

Chapter 4 of this work has been published as Domenico Giuliano, Phong H. Nguyen, Andrea Nava, and Massimo Boninsegni, "Uniaxial modulation and the Berezinskii-Kosterlitz-Thouless transition", ArXiv:2302.10335 (2023).

Chapter 5 of this work has been published as Phong H. Nguyen and Massimo Boninsegni, "Phase diagram of hard core bosons with anisotropic interactions", Journal of Low Temperature Physics **209**, 34 (2022).

All of the papers listed are collaborative works between individuals who contributed equally to the writing and research effort. The codes used in Chapter 3 and Chapter 4 were written by myself, while the code used in Chapter 5 was written by Dr. Lode Pollet.

Acknowledgements

First and foremost, I would like to express my deep gratitude to my supervisor, Professor Massimo Boninsegni, for his patience, motivation, and especially his enthusiasm for physics, which encourage me to do my research. Without his guidance and patient dedication, none of this work would have been possible.

Furthermore, I wish to thank Professor Lode Pollet, for his help with the numerical technique that was instrumental to the completion of the work in Chapter 5.

I would also like to acknowledge the beneficial collaboration with Professor Domenico Giuliano and Andrea Nava, for their analytical support.

Finally, the support from the Natural Science and Engineering Research Council of Canada (NSERC) grant and Computing support from ComputeCanada are gratefully appreciated.

Table of Contents

List of Figures

Chapter 1

Introduction

In 1937, one of the most spectacular manifestations of quantum mechanics was discovered, which still drives much fundamental research in condensed matter physics. This is the phenomenon of *superfluidity*, namely the ability of a substance to sustain persistent, dissipation-less flow. It was first observed independently by Kapitza [1], and by Allen and Misener [2]. Specifically, there is a phase transition in liquid ^{4}He, occurring at a temperature $T_\lambda \approx 2.17K$ at saturated vapor pressure. Above this temperature, ^{4}He (which liquefies at 4.2 K under the pressure of its own vapor) behaves as an ordinary, viscous fluid, while below T_λ it can flow with essentially no viscosity.

Shortly after the discovery of superfluidity in liquid ^{4}He, Tisza proposed the helpful, two-fluid phenomenological model [3], which is still widely adopted to interpret the phenomenology and guide the theoretical study of superfluidity, not just in helium but in any other superfluid system. According to it, at temperature $T < T_\lambda$, liquid ^{4}He comprises two components, namely the *normal* one, which is viscous, and the *superfluid*, which carries no entropy and flows without dissipation. In a translationally invariant system, the superfluid component dominates and constitutes 100% of the system in the $T \to 0$ limit. On the other hand, if the system breaks translational invariance, a finite normal component remains present even $T = 0$ [4].

The subject of superfluidity (SF) continues to intrigue theorists and experimenters, first of all for its fundamental importance and its broad relevance to, e.g., supercon-

ductivity, a topic of great (also potentially applied) interest, but also because there are still a number of aspects that remain to be elucidated. These include, and are not limited to, the possible simultaneous presence of SF with structural long-range order and the evolution of the superfluid properties of a system as its effective dimensionality is varied. Indeed, over the past few decades, much progress has been made in the understanding of how SF manifests itself in reduced dimensions.

In three dimensions (3D), SF occurs alongside Bose-Einstein Condensation (BEC), a collective phenomenon that is related to a specific type of quantum statistics (Bose) obeyed by the elementary constituent particles of the system, which have integer spin, and the relationship between the two phenomena is now well understood [5]; indeed, experimental evidence shows that the onset of SF is concomitant with that of BEC in liquid ^{4}He, as the single-particle momentum distribution $n(k)$ displays a δ-like peak at $k = 0$, signaling macroscopic occupation of the same ($\mathbf{k}$=0) single-particle state. Concurrently (and equivalently), the one-body density matrix, which decays exponentially at temperature above T_λ, at lower temperatures plateaus at a finite value $n_\circ(T)$, known as the *condensate fraction* (see, for instance, Ref. [6]).

Additional evidence of the connection between BEC and SF comes from superconductivity in Fermi systems, which is underlain by the formation of (Cooper) pairs of particles of half-integer spin, which form composite objects of integer spin, obeying Bose statistics and thus undergoing BEC. Indeed, superconductors are essentially charged superfluid [6]. In 3D, superfluidity is in essence a macroscopic manifestation of quantum particles behaving collectively as classical complex fields [7]. This behavior, which is made possible by Bose statistics, was until recently thought to be observable only in systems comprising a macroscopically large number of particles [8–10], but spectroscopy of solvated linear molecules in ^{4}He nano-droplets has shown that in fact evidence of SF can be obtained even in systems with as few as ~ 7 ^{4}He atoms [11].

In two dimensions (2D), on the other hand, the theoretical picture is modified, as no

BEC can occur at any finite temperature [12]. In this case, a superfluid transition can still occur at a finite temperature T_{BKT}, below which the one-body density matrix decays algebraically; at $T = T_{BKT}$, the fraction of the system that is superfluid, henceforth referred to as $\rho_S(T)$, "jumps" to a finite value, in contrast to the 3D case where it grows smoothly below T_λ. The framework describing theoretically the superfluid transition in 2D is known as the Berezinskii-Kosterlitz-Thouless (BKT) formalism [7, 13–16].

Yet another change occurs as the dimensionality is lowered to 1D, in which the low-energy, long-wavelength dynamics is described by the "universal" harmonic Tomonaga-Luttinger liquid (TLL) theory [17], making stringent predictions on the behavior of several observable quantities. For instance, while no true SF can occur at any finite temperature in the thermodynamic limit, SF manifests itself as a *finite-size effect*. According to the TLL theory, the superfluid fraction $\rho_S(L, T)$, where L is the linear size of the system, is a universal function of LT/v, where v is the superfluid velocity. In this case, the one-body density matrix displays a power-law decay modulated by oscillations reflecting the atomic nature of the fluid at the microscopic scale [18].

In spite of these differences, the unifying concept of classical complex field allows one to study some aspects of the superfluid transition in *any* dimensions by considering *classical* field theories, including some that are defined not in continuous space but on a discrete lattice. For example, a classical planar spin model such as the x-y can describe many of the thermodynamic properties of the superfluid transition in 3D and 2D, as it is in the same *universality class* [19] as the corresponding superfluid systems, even though these obey the laws of quantum mechanics. Without embarking into a formal discussion of this subject, this is due to the fact a phase transition such as the superfluid one ultimately involves the onset of *long range order* (in this case off-diagonal), which extends over macroscopic distances. In these conditions, quantum, classical, continuous and lattice theories yield the same predictions for aspects such as the behavior of the order parameter as a function of temperature, the order

of the phase transition, critical exponents, etc.

Taking advantage of this fundamental theoretical result, we address in this thesis some aspects of the superfluid transition in reduced dimensions and/or in the presence of external modulating fields, making use of classical and quantum lattice models. A major justification for taking this particular route is that relatively new computational methods are now available, such as the Worm Algorithm in the lattice flow representation [20], which allow one to investigate with essentially arbitrary accuracy general models of classical and quantum statistical mechanics, yielding robust quantitative predictions valid in the thermodynamic limit. It should be noted that the study of how a quantum fluid behaves in reduced dimensions is still a topic of much research, mainly due to recent advancements in technology that allow for the investigation of new and uncharted areas such as thin films of superfluid helium or cold atom assemblies.

One of our goals is gaining an understanding of the behavior of the specific heat in a 2D superfluid, which is still poorly understood (this has led to a number of conflicting and contradictory interpretations of experimental results for ^{4}He films). While in 3D the specific heat displays a sharp peak in correspondence with the superfluid transition, it is unclear whether such an anomaly occurs in 2D.

Existing theoretical predictions, almost exclusively based on computer simulations [21, 22] are inconclusive, largely due to the small size of the systems simulated. The results suggest an anomaly in the specific heat, possibly evolving either into a cusp [23] or disappearing altogether in the thermodynamic limit and/or at a temperature different from T_{BKT}. In this work, we have addressed this issue by carrying out extensive numerical simulations of the 2D classical x-y model based on state-of-the-art methodology, never utilized before and capable of handling much larger system sizes than those previously studied. Our main finding is that the position and the shape of the peak survive in the thermodynamic limit, but the peak does not turn into a cusp. Rather, it remains a fairly broad anomaly, not signaling the occurrence

of any phase transition [24].

We also address the issue of possible dimensional crossover in the presence of strong external modulating potentials. An interesting theoretical question raised by these studies is whether it is possible to alter the effective dimensionality of a superfluid by varying some external parameters and observing how it affects the system's behavior [25]. For example, one might think of inducing a dimensional crossover by superimposing, e.g. to a 2D system, an external modulating potential of variable amplitude *along a specific direction*. An experiment along these lines, feasible with, e.g., current cold atom technology [26–28], should show the system breaking down into almost independent, quasi-1D stripes (or "tubes"), when the external potential is strong enough. This could be accompanied by a change in the system's dimensionality from 2D to 1D.

We study the possible dimensional crossover in a 2D superfluid in the presence of an external potential, imparting to the system in just one direction, in the context of the classical $|\psi|^4$ field theory, which falls in the same universality class of a 2D superfluid and is a generalization of the x-y model that allows for fluctuations of the local density of the system. Our main finding is that the system remains 2D in character, i.e., no dimensional crossover takes place. Overall, we find that the $|\psi|^4$ model in the presence of an external modulation along one direction behaves similarly to the anisotropic x-y model.

Finally, an intriguing subject attracting a lot of current theoretical and experimental research is centered on the search for an exotic phase of matter, in which superfluidity and crystalline long-range order coexist in a single homogeneous phase, called *supersolid*. More than 50 years ago, Andreev and Lifshitz first suggested the possibility of a supersolid phase, which would exhibit crystalline order (rigid, or diagonal long-range order with broken translation symmetry) and superfluidity [29]. The effort to find this intriguing phase of matter has mainly been directed toward solid helium, however, new possibilities for its discovery are emerging, particularly in

the field of cold atom physics. Recently, a valuable understanding of the potential existence of a supersolid phase has been provided from the investigation of lattice hard-core bosons [30–38]. This is a minimal model of a strongly interacting system displaying a superfluid phase at low temperature, as well as a quantum phase transition between superfluid and crystalline ground states. It is also believed that the primarily dipolar interaction, i.e., anisotropic interaction, in principle can stabilize different crystalline and/or superfluid phases, breaking rotational symmetry. Moreover, an interesting theoretical question is raised regarding the significance of the long range of the interaction in stabilizing specific, exotic thermodynamic phases, e.g., the supersolid.

In this work, we study the phase diagram of a system of hard-core bosons on the square lattice, interacting via an anisotropic nearest-neighbor potential, with the repulsive interaction in one direction and the attractive interaction in the other [39]. We map out the complete finite temperature phase diagram, which is qualitatively very similar to that of a system of hard-core dipolar bosons with aligned dipole moments, tilted with respect to the perpendicular to the plane. Our main result is that no supersolid phase exists in this model, and that long-range interactions do not bring about any substantially new physics with respect to what can be observed in a system with short-range interactions only. The computational methodology utilized in this project is the Worm Algorithm in the lattice path-integral representation [40, 41], which is a Quantum Monte Carlo (QMC) technique widely regarded as the method of choice to study equilibrium thermodynamic properties of Bose systems at a finite temperature.

This thesis is organized as follows: in Chapter 2 we briefly review the methods utilized to study the systems of interest. Because these methods are extensively described in the literature, we only sketch their basic features. In Chapter 3, we discuss our work on the superfluid transition and the specific heat of the 2D classical x-y model on the square lattice. In Chapter 4, we present our study of the superfluid

transition of the classical $|\psi|^4$ field theory in 2D, in the presence of an external potential, imparting to the system in just one direction. Then, in Chapter 5, we describe the phase diagram of lattice hard-core bosons with anisotropic interactions. Finally, our conclusions are outlined in Chapter 6.

Chapter 2

Methodology

2.1 Classical Worm Algorithms for lattice models

In this section, we briefly review the methodology, which will be used to perform large-scale computer simulations in Chapters 3 and 4. This is the Worm algorithm (WA) in high-temperature expansion and the lattice flow representation. This methodology was first introduced by Nikolay Prokof'ev and Boris Svistunov in 2001 and showed a fantastic performance; in particular, it has been demonstrated not to suffer from the well-known "critical slowing down" that affects existing local update schemes, while at the same time retaining their simplicity, i.e., not requiring the complexity of cluster updates [20].

We provide here a brief illustration of the classical worm algorithm, using the $|\psi|^4$ model on the square lattice as a simple example, which is however general enough to encompass all of the cases studied in this work. Considering a square lattice of $N = L \times L$ sites, the Hamiltonian of this model is expressed as follows:

$$H = -t \sum_{\langle ij \rangle} [\psi_i^* \psi_j + \psi_i \psi_j^*] - c \sum_i |\psi_i|^2 + \frac{U}{2} \sum_i |\psi_i|^4 \tag{2.1}$$

where ψ_i is a complex variable at lattice site i, t is the particle hopping energy between the nearest neighbor sites, c is the chemical potential, and U is an on-site interaction between particles.

The partition function of this model reads[1]

$$Z = \int d\psi_1 \; d\psi_1 \; ... \; d\psi_N \; e^{-H/T} \tag{2.2}$$

On expanding the exponentials associated with the first two terms of Equation (2.1) into series one can write

$$Z = \sum_{\{n_b, m_b\}} \left(\prod_b \frac{(t/T)^{n_b+m_b}}{n_b! m_b!} \right) \prod_i \left(\int d\psi_i \; \psi_i^{p_i} \; (\psi_i^*)^{r_i} \; e^{-(U/2T)|\psi_i|^4 + (c/T)|\psi_i|^2} \right) \tag{2.3}$$

where n_b (m_b) are powers pertaining to a specific (i, j) bond (indicated by b), the first product is over all bonds, and p_i, r_i are the sum of all powers associated to bonds that include the site i. We can now express the integrals in Equation (2.3) over the complex fields in polar coordinates, i.e.,

$$\begin{aligned} &\int d\psi \; \psi^p \; (\psi^*)^r \; e^{-(U/2T)|\psi|^4 + (c/T)|\psi|^2} = \\ &\int d|\psi| |\psi|^{p+r+1} e^{-(U/2T)|\psi|^4 + (c/T)|\psi|^2} \int d\phi \; e^{i\phi(p-r)} \end{aligned} \tag{2.4}$$

It is obvious that the phase integral in Eq. (2.4) is only non-zero when $p = r$; this means that the sum in Equation (2.3) only includes terms for which the powers n_b, m_b add up to the same value for each lattice site. This suggests a graphical representation of Equation (2.3), in which the term $(\psi_i^* \psi_j)$ (corresponding to the hopping of a particle from site i to site j) can be associated with a directed arrow $\rightarrow$ from site i to site j, and the term $(\psi_i \psi_j^*)$ can be associated with the opposite arrow $\leftarrow$. These directed arrows are called currents. Thus, p_i (r_i) is the net incoming (outgoing) current at site i, and the partition function extends over all current loops such that the net current at each site is zero.

If the configuration space of the model can be seen as the set of all possible closed loops, then the process of generating these oriented loops corresponds to drawing with a pencil along the bonds of a square lattice, without ever detaching the tip of the pencil from the sheet, until one closes the loop.

[1] We set the Boltzmann constant $k_B = 1$ throughout this whole document

Because $p = r$, Equation (2.4) can be written as a function of p:

$$Q(p) = \int_{-\infty}^{\infty} dx \; x^{2p+1} e^{-(U/2T)x^4 + (c/T)x^2} \tag{2.5}$$

The weight of a configuration can be written as follows:

$$W(\{n_b, m_b\}) = \prod_b \left(\frac{(t/T)^{n_b+m_b}}{n_b! m_b!} \right) \prod_i Q(p_i) \tag{2.6}$$

The partition function now becomes:

$$Z = \sum W(\{n_b, m_b\}) \tag{2.7}$$

with the sum runs over closed directed loops. Therefore, the partition function Z (2.7) can be sampled according to the weight function $W(\{n_b, m_b\})$ in a closed-loop configuration in which it is distributed. The procedure to sample random configurations defined in this way, suitable to evaluate thermodynamic averages statistically, is very simple, and is described in Ref. [20]. The computer codes utilized in this thesis work were written by me, based on those prescriptions.

Consider now some estimators of interest. First, the thermal average of the energy is given by

$$\langle E \rangle = -\frac{1}{Z} \frac{\partial Z}{\partial(\frac{1}{T})} = -T \langle n_b + m_b \rangle \tag{2.8}$$

We also have:

$$\langle E^2 \rangle = \frac{1}{Z} \frac{\partial^2 Z}{\partial(\frac{1}{T})^2} = T^2 \langle (n_b + m_b)^2 - (n_b + m_b) \rangle \tag{2.9}$$

Using Equations (2.8) and (2.9), we can derive the specific heat:

$$C = \frac{1}{T^2} (\langle E^2 \rangle - \langle E \rangle^2) = \langle (n_b + m_b)^2 - (n_b + m_b) \rangle - \langle n_b + m_b \rangle^2 \tag{2.10}$$

Another important estimator that we consider is the superfluid density ρ_S. In a classical field theory, this quantity is equivalent to the helicity modulus [19], which is related to the change in the free energy of the system per unit length due to a shift applied to the phases along either direction. This allows one to obtain an estimator

for the superfluid density known as the winding number M_x [42], which counts the number of times single-particle paths "wrap" around periodic boundary conditions:

$$M_x = L_x^{-1} \sum_{b=(i,\hat{x})} (n_b - m_b) \tag{2.11}$$

Within the scheme described above for the classical field theory of interest here, the estimator of the superfluid density is expressed as follows:

$$\rho_S = \frac{T}{t} \frac{L^{2-d}}{d} \langle M^2 \rangle \tag{2.12}$$

where d is the dimensionality, and L is the linear size of the system.

Finally, we can also compute the correlation function

$$g(l, m) = \langle \psi_l^* \psi_m \rangle \tag{2.13}$$

This quantity can be shown [20] to be obtained as a "by-product" of the scheme that generates configurations of closed loops, which, as mentioned above, are those that contribute to the partition function. On the other hand, one can also consider intermediate configurations, with one open loop, in which there exist two "dangling" ends. These configurations contribute to the correlation function given by Equation (2.13), which is obtained simply by histogramming the frequency with which the two dangling ends are at a distance $l - m$, in the course of the simulation (obviously, for any system that is isotropic and translationally invariant, $g(l, m) \equiv g(|l - m|)$).

The above methodology is quite general, and the formulation based on the $|\psi|^4$ field theory can be straightforwardly shown to encompass a broad array of similar lattice models. One of these is the x-y model, which is the subject of one of the projects described in this thesis, and which is a limiting case of the $|\psi|^4$ theory, approached when $U = c \to \infty$.

2.2 Worm Algorithm for lattice bosons

In this section, the methodology utilized to investigate the phase diagram of a system of hard core bosons in Chapter 5 is briefly reviewed. This is the Worm Algorithm in

the lattice path-integral representation [40], specifically its implementation described in Ref. [41]. Just like for the above case, we begin by introducing a paradigmatic Hamiltonian, specifically that of the Bose-Hubbard Model:

$$\hat{H} = \hat{T} + \hat{V}, \text{ with } \hat{T} = -t \sum_{\langle ij \rangle} (\hat{b}_i^\dagger \hat{b}_j + h.c.), \ \hat{V} = U \sum_i \hat{n}_i^2 \tag{2.14}$$

Just like for Equation (2.1), the sum $\sum_{\langle ij \rangle}$ runs over all pairs of nearest-neighboring sites of a lattice (for simplicity assumed square), t is a nearest-neighboring particle hopping integral and U is the on-site interaction between particles; the operator $\hat{b}_i^\dagger(\hat{b}_i)$ is the standard Bose creation (annihilation) operator at lattice site i, and $\hat{n}_i \equiv \hat{b}_i^\dagger \hat{b}_i$ is the number operator.

The similarity between Equation (2.14) and Equation (2.1) is evident, and certainly not accidental. Indeed, it can be shown that Equation (2.1) is the *classical limit* of Equation (2.19), approached when $\langle \hat{n}_i \rangle >> 1$, $\langle .. \rangle$ standing for thermal average.

For a physical system in thermal equilibrium at temperature T, the thermal average of an observable, represented by a quantum-mechanical operator $\hat{O}$, can be determined as

$$\langle \hat{O} \rangle = \frac{Tr\{\hat{O}\hat{\rho}\}}{Tr\{\hat{\rho}\}} \tag{2.15}$$

Here, we assume to be in the grand canonical ensemble, in which the total number N of particles can fluctuate around a mean. Thus, $\hat{\rho} = e^{-\beta \hat{K}}$, with $\beta \equiv (1/T)$, $\hat{K} = \hat{H} - \mu \hat{N}$ is the "Grand Canonical" Hamiltonian and μ is the chemical potential. The Grand Canonical partition function Ξ reads

$$\Xi = Tr\{\hat{\rho}\} = \sum_{N=0}^{\infty} e^{\beta \mu N} Z_N \tag{2.16}$$

in which Z_N is the Canonical partition function for the sector of configurations with N particles, i.e.,

$$Z_N = Tr\{\hat{\rho}_N\} = \sum_c \langle c | \hat{\rho}_N | c \rangle \tag{2.17}$$

with $\hat{\rho}_N = e^{-\beta \hat{H}}$, and $|c\rangle \equiv |\{n_i\}\rangle$ is a generic basis state in the site occupation representation (with $\sum_i n_i = N$).

Following the same approach that leads to Dyson's series solution of the time-dependent[2] Schrödinger's equation [43], we consider the off-diagonal operator $\hat{T}$ as a "perturbation", and $\hat{V}$ as the "unperturbed" Hamiltonian. As a result, $\hat{\rho}_N$ can be expressed as follows:

$$\hat{\rho}_N = e^{-\beta\hat{H}} = e^{-\beta\hat{V}}\ \hat{\mathcal{T}}\exp\left[-\int_0^\beta \hat{T}(\tau)d\tau\right] \tag{2.18}$$

where $\hat{T}(\tau) = e^{\tau\hat{V}}\hat{T}e^{-\tau\hat{V}}$, and $\hat{\mathcal{T}}$ is the time-ordering operator, i.e.,

$$\begin{aligned}\hat{\mathcal{T}}\exp\left[-\int_0^\beta \hat{T}(\tau)d\tau\right] &= 1 - \int_0^\beta \hat{T}(\tau)d\tau + \int_0^\beta d\tau_1 \int_0^{\tau_1} d\tau_2 \hat{T}(\tau_1)\hat{T}(\tau_2) - ... \\ &= \sum_{n=0}^{\infty}(-1)^n \int_0^\beta d\tau_1 \int_0^{\tau_1} d\tau_2 ... \int_0^{\tau_{n-1}} d\tau_n\ \hat{T}(\tau_1)...\hat{T}(\tau_n)\end{aligned} \tag{2.19}$$

Now the canonical partition function (2.17) can be written as:

$$\begin{aligned}Z_N &= Tr\ e^{-\beta\hat{V}} \sum_{n=0}^{\infty}\int_0^\beta d\tau_1 \int_0^{\tau_1} d\tau_2 ... \int_0^{\tau_{n-1}} d\tau_n \hat{T}(\tau_1)...\hat{T}(\tau_n) \\ &= \sum_c \langle c|e^{-\beta\hat{V}} \sum_{n=0}^{\infty}\int_0^\beta d\tau_1 \int_0^{\tau_1} d\tau_2 ... \int_0^{\tau_{n-1}} d\tau_n \hat{T}(\tau_1)...\hat{T}(\tau_n)|c\rangle \\ &= \sum_{\{c_0,...,c_{n-1}\}} \langle c_0|\hat{T}|c_{n-1}\rangle\langle c_{n-1}|\hat{T}|c_{n-2}\rangle ...\langle c_1|\hat{T}|c_0 \equiv c_n\rangle \times \int_0^\beta d\tau_1 \int_0^{\tau_1} d\tau_2 \\ &... \int_0^{\tau_{n-1}} d\tau_n e^{-(\beta-\tau_1)\hat{V}(c_1)} e^{-(\tau_1-\tau_2)\hat{V}(c_2)} ... e^{-(\tau_{n-2}-\tau_{n-1})\hat{V}(c_{n-1})} e^{-\tau_{n-1}\hat{V}(c_0)}\end{aligned} \tag{2.20}$$

where we have inserted sums over complete sets, $\sum_c |c\rangle\langle c| = 1$, between all of the operators $\hat{T}$. Because we are determining the *trace*, the constraint $c_0 \equiv c_n$ must be satisfied. Since hopping terms in $\hat{T}$ vary the state by moving only one particle to a nearest-neighbor site, the sequence of matrix elements in $\hat{T}$ can be identified by specifying the "imaginary time trajectory" of occupation numbers $\{n_i(\tau)\}$. Hence, the canonical partition function Z_N can be considered as a sum over all possible paths $\{n_i(\tau)\}$ satisfying $n_i(\beta) = n_i(0)$, i.e.,

$$Z_N = \sum_{n=0}^{\infty}\int_0^\beta d\tau_1 \int_0^{\tau_1} d\tau_2 ... \int_0^{\tau_{n-1}} d\tau_n \sum_{\{n_i(\tau)\}} W_n(\{n_i(\tau)\}) \tag{2.21}$$

[2]It should be noted that $\beta\hbar$ has units of time, and therefore is often referred to as "imaginary time", in analogy with the time evolution operator $e^{-i\hat{H}t/\hbar}$.

where $W_n(\{n_i(\tau)\})$ is the weight of a generic configuration, which reads:

$$W_n(\{n_i(\tau)\}) = (\beta t)^n \exp\left[- \int_{\tau=0}^{\beta} d\tau \hat{V}\{c(\tau)\} \right] \tag{2.22}$$

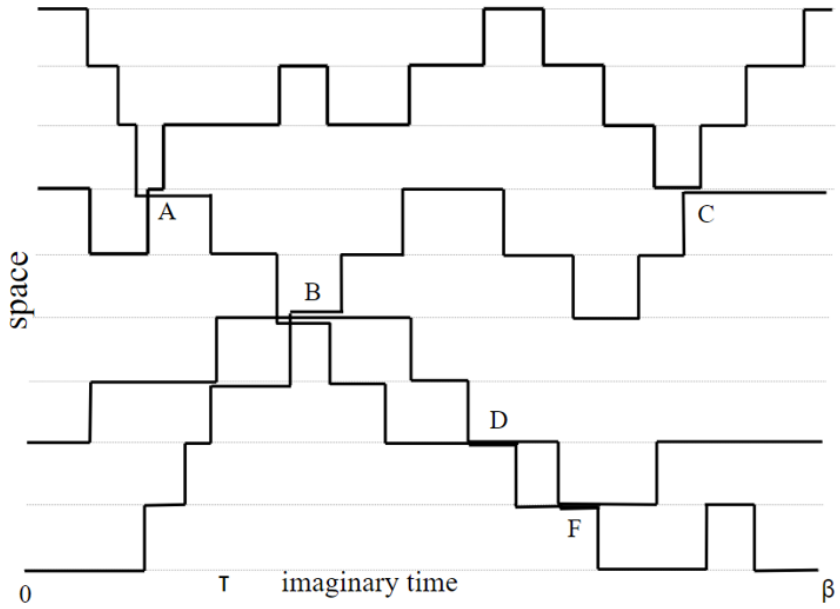

Figure 2.1: An example of world line representation for a one-dimensional system.

Because of the particle number conservation, the many-body trajectory can be decomposed into a set of closed (in the time direction) single-particle trajectories, or world lines. Indeed, the contribution of order n is represented by n "kinks" (hopping events) occurring at different times, and integral over all many-particle paths features an arbitrary number of "kinks".

Therefore, the canonical partition function Z_N (2.21) can be sampled by sampling closed paths with arbitrary numbers of "kinks" at varying consecutive ordered times according to the weight function $W_n(\{n_i(\tau)\})$. This sampling procedure is graphically very similar to that of the classical field theory described above. Moreover, one can vary the number of particles inserting or deleting particles with probability proportional to $e^{\pm\beta\mu}$.

The procedure to sample random configurations defined in this way, suitable to evaluate thermodynamic averages statistically, is described in Ref. [40, 41]. The

computer code utilized in this thesis work was provided by Lode Pollet [41].

The physical quantities of interest are the superfluid density ρ_S (which is computed by Equation (2.12)), and the static structure factor $S(\mathbf{Q})$, which for a square lattice of $L \times L$ sites is defined as

$$S(\mathbf{Q}) = \frac{1}{L^4} \left\langle \left| \sum_{i=1}^{L^2} \hat{n}_i \; e^{i\mathbf{Q}\cdot\mathbf{r}_i} \right|^2 \right\rangle \tag{2.23}$$

If the physical system features crystal order, the quantity $S(\mathbf{Q})$ displays (Bragg) peaks at reciprocal lattice vectors $\mathbf{Q}$. It therefore allows us to distinguish a crystalline phase versus one that does not possess density long-range order.

Chapter 3

Superfluid transition and specific heat of the 2D x-y model

In this chapter, we present our study on the behavior of the superfluid transition and the specific heat of the 2D classical x-y model on the square lattice [24].

3.1 Introduction

The two-dimensional classical x-y model is the simplest model to display a Kosterlitz-Thouless (KT) transition [7, 14–16]. Also falling in the KT universality class, the superfluid phase transition in two dimensions (2D) is the focus of continuing experimental and theoretical research, particularly in the setting of thin films of ^{4}He adsorbed on a wide variety of substrates [44–49]. The x-y model is studied theoretically, often using computer simulations, in order to determine whether a particular physical system being studied belongs to the same universality class as described by the KT paradigm, and to predict the behavior of other systems that have not yet been explored [50–53]. Decades of computer simulation studies of the 2D x-y model, conducted on square lattices as large as $L = 2^{16}$ [54], have been used to accurately estimate the temperature at which superfluidity occurs (T_c) and the critical exponents related to the transition [22, 23, 54–60].

The behavior of the specific heat has received less attention, which exhibits an anomaly at a temperature $\sim 17\%$ above Tc in numerical simulations of the x-y model

on square lattices of size $L = 2^8$ [22]. Although the size of the simulated lattice appears to have little influence on the peak's position, to our knowledge, no systematic research has been done to determine whether or not such an anomaly exists in the thermodynamic limit and where exactly it is. There have been also speculations that the peak's width may shrink in the thermodynamic limit and the peak itself might turn into a cusp [23]. Such an anomaly does not seem to indicate the occurrence of any phase transition, and there is currently no agreement on the physical interpretation of it. Interestingly, experiments on ^{4}He monolayers [61], as well as computer simulations [62] (including of 2D ^{4}He [21]) have also yielded evidence of a peak in the specific heat at temperature *above* the superfluid transition temperature.

As far as we know, no additional studies of the specific heat have been conducted to examine how the temperature of the peak shifts and how the overall shape of the curve changes as the lattice size increases, beyond that of Ref. [22]. One reason for the lack of further study in this area is that calculating the specific heat using direct numerical (Monte Carlo) simulations can be prone to significant statistical uncertainty due to the inherent "noisiness" of current specific heat estimators. However, in the almost three decades since the publication of Ref. [22], there have been significant advances in both computing power and simulation techniques that may make it more feasible to conduct more accurate and efficient simulations. It would be useful to reconsider this topic, which has the potential to be relevant to experiments, as the x-y model is sometimes used to explain measurements of the specific heat of thin films of ^{4}He, and also to make predictions in the same context [52, 53].

In this chapter, the simulations on square lattices of size up to $L = 2^{12}$ are carried out. The main goal of our research is to thoroughly examine the specific heat and provide reliable information about how it behaves in the thermodynamic limit. To confirm the validity of our study, we also calculated the superfluid transition temperature and spin correlations, and compared them to the most recent theoretical estimates. Our calculation of T_c agrees with the most accurate published result to

date, which is found in Ref. [54]. Our numerical results provide strong evidence that the specific heat anomaly exists in the thermodynamic limit and its shape remains essentially unchanged with respect to that on a lattice of size $L = 2^8$. We estimate the position of the peak of the specific heat in the thermodynamic limit to be at temperature 1.043(4) (in units of the coupling constant).

The remainder of this chapter is organized as follows: in Section 3.2 we describe the model of the system. In Section 3.3 we present and discuss our results, and we finally outline our conclusions in Section 3.4.

3.2 Model

The Hamiltonian of the classical x-y model is given by

$$H = -J \sum_{\langle ij \rangle} \mathbf{s}_i \cdot \mathbf{s}_j \tag{3.1}$$

The sum in this equation is over all pairs of nearest-neighboring sites, and $\mathbf{s}_i \equiv s(\cos\theta_i,\ \sin\theta_i)$ represents a classical spin variable associated with site i. The equation is considering a square lattice of $N = L \times L$ sites with periodic boundary conditions. For the purposes of this work, the energy and temperature are expressed in units of Js^2. To study the behavior of the model at low temperatures, we use classical Monte Carlo simulations, a method that is described in detail in Ref. [20]. The details of our calculations are standard.

As previously mentioned, a significant aspect of this research involves examining the superfluid transition in order to compare our results with those of other studies and assess the accuracy of our methodology. We determine the superfluid transition temperature T_c using two different ways. The first consists of computing the superfluid fraction $\rho_s(L, T)$ on a lattice of size L, as a function of temperature, using the well-known winding number estimator [42]. We then determine a size-dependent transition

temperature $T_c(L)$ based on the universal jump condition [63]

$$\rho_s(L, T_c) = f_r \ \frac{2T_c}{\pi} \tag{3.2}$$

where $f_r = 1 - 16\pi e^{-4\pi}$ [64]. Equation (3.2) can be used to obtain an estimate of the transition temperature ($T_c(L)$) on a lattice of finite size. In order to extrapolate the value of $T_c(L)$ to the thermodynamic ($L \to \infty$) limit (referred to as T_c), we fit the results for $T_c(L)$, obtained for different system sizes to the expression [65]:

$$T_c(L) = T_c + \frac{a}{(\ln bL)^2} \tag{3.3}$$

where a, b are constant. It should be noted that other expressions have been proposed, aimed at extracting T_c [60]; we will address this issue further when discussing the results of our study.

It is also possible to determine the superfluid transition temperature by analyzing the behavior of the spin correlation function [66], particularly the way in which the correlation length ξ diverges as $T \to T_c$, namely [7, 14, 15]:

$$\xi(T) \sim A \ e^{\frac{c}{\sqrt{t}}} \tag{3.4}$$

where A, c are constant ($c \approx 1.5$ [66]), and $t = \frac{(T - T_c)}{T_c}$ is the reduced temperature. The correlation length $\xi(T)$ at a temperature above the critical temperature T_c, can be found using a simple fitting procedure on the computed correlation function, illustrated in Ref. [55]. Using the best fit to Equation (3.4), an estimate of T_c is obtained; as the size of the system increases, the estimated T_c becomes more accurate. The estimates of T_c obtained using the two methods described above are consistent within their statistical uncertainties, but the first method, which relies on the universal jump of the superfluid fraction, gives a more precise determination of T_c.

Moreover, we calculate the specific heat (i.e., the heat capacity per site) through the direct estimator of the heat capacity [67], based on the mean-squared fluctuations of the total energy E:

$$C = \frac{1}{L^2}\beta^2(\langle E^2 \rangle - \langle E \rangle^2), \tag{3.5}$$

where $\beta = 1/T$ is the inverse temperature. This estimator is numerically "noisy", and because of this, it is common to use numerical differentiation of the energy values with respect to temperature as an alternative [55]. However, in our case, accurate estimates of the specific heat can be obtained reasonably using Equation (3.5), thanks to the available computing facilities and the methodology adopted.

3.3 Results

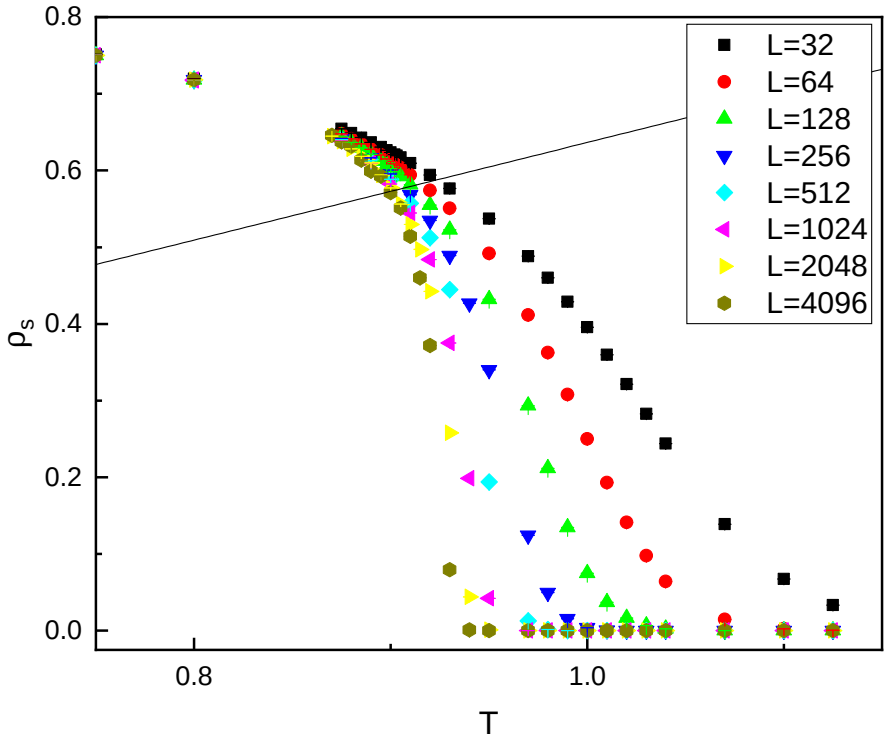

Figure 3.1: The superfluid fraction ρ_s versus temperature, for the different lattice sizes considered. Statistical errors are smaller than symbol sizes. The straight line corresponds to the universal jump condition (right hand side of Equation (3.2))

We start by showing how the superfluid fraction varies with temperature for different lattice sizes, and then we discuss how we determined the transition temperature and compare it to those found in other studies. Figure 3.1 shows the computed value

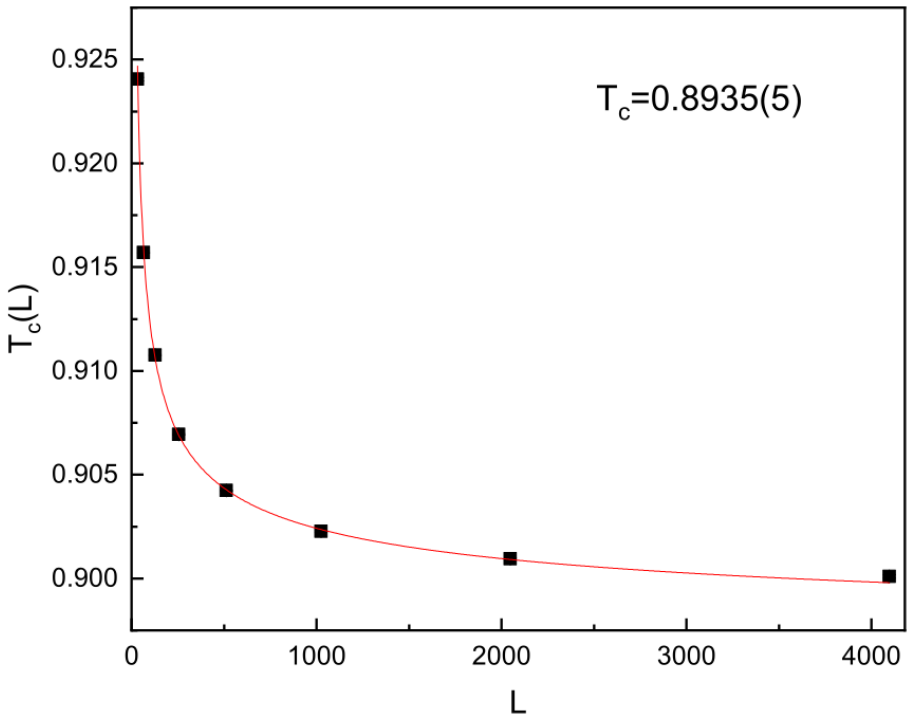

Figure 3.2: The critical temperature $T_c(L)$ versus the system size L. Solid line is a fit to the data using Equation (3.3).

of $\rho_s(L,T)$; the critical temperature $T_c(L)$ for a given system size is determined by the universal jump condition, namely the intersection of the $\rho_s(L,T)$ curve with the straight line given by the right-hand side of Equation (3.2). To estimate the intersection point, we draw a straight line between the two adjacent values of $\rho_s(L,T)$ that we can be confident the intersection occurs within, based on the accuracy of our calculation.

As expected, both $T_c(L)$ and $\rho_s(L,T_c(L))$ gradually decrease as L increases. In order to extrapolate the value of T_c in the thermodynamic ($L \to \infty$) limit, we use Equation (3.3) to fit the calculated $T_c(L)$, as proposed in Ref. [54]. This procedure is illustrated in Figure 3.2. According to our calculations, the value of T_c is 0.8935(5). This result is in agreement with the value from another study, Ref. [54], which is 0.89289(5). Despite the fact that the uncertainty in their value is much smaller than ours, their system sizes were significantly larger (16 times larger), which could

account for the difference in uncertainty. Our estimate of T_c also agrees exactly with a more recent study, Ref. [60], which used the same computational method as ours and examined the same system sizes. The precision of their results is similar to ours. While they used a different, more complex fitting form for $T_c(L)$, their final estimate for T_c is consistent with ours and has the same level of uncertainty.

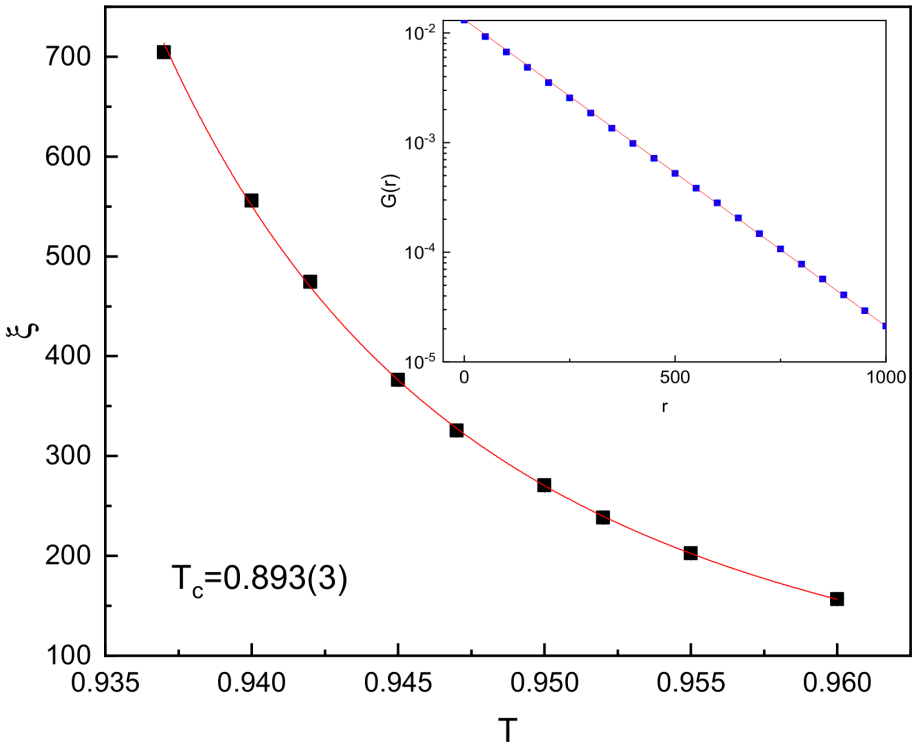

Figure 3.3: The correlation length ξ as a function of the temperature, for a system of size $L = 4096$. The solid line is a fit to the data using expression (Equation (3.4)). Inset shows the computed spin correlation function $G(r)$ for a temperature $T = 0.96$.

As mentioned in Section 3.2, as a way to verify our results, we also estimated the critical temperature T_c by independently analyzing the spin correlation length. To determine T_c using the spin correlation function, we first extract the temperature-dependent correlation length $\xi(T)$ and then fit the results to Equation (3.4). This process gives us an estimate of T_c for a particular system size. An example of this procedure is shown in Figure 3.3, for the largest system size considered here, which is the one that gives us the most precise estimate of T_c. Such an estimate, namely

0.893(3), is in agreement with the estimate obtained from the superfluid fraction, but it is considerably less precise.

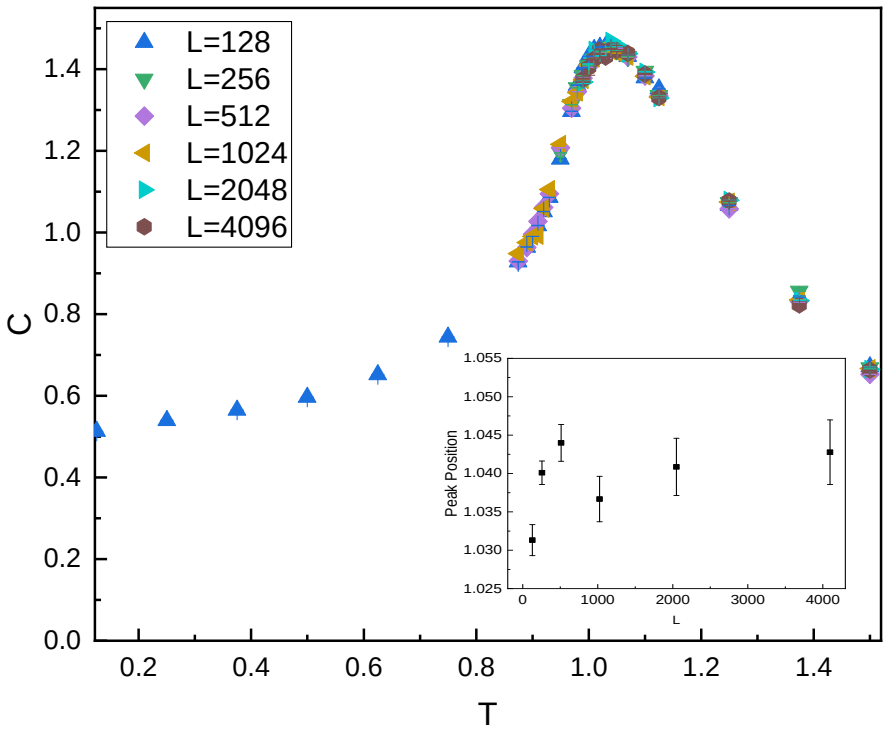

Figure 3.4: The specific heat C versus the temperature T for different lattice sizes. The inset shows the position of the peak as a function of lattice size.

Since our result for T_c gives us confidence in the reliability of our data and simulation, we now discuss the main focus of this chapter, which is the behavior of the specific heat $C(T)$. It is worth mentioning that earlier numerical studies of the 2D x-y model [22, 55] have only produced results for the specific heat $C(T)$ for square lattices with sizes up to $L = 256$. Such studies yielded evidence of a peak in the specific heat at a temperature above T_c; the position of this peak depends fairly strongly on system size for $L \leq 128$. However, the shape of $C(T)$ seems to change little when going from $L = 128$ to $L = 256$, which suggests that the anomaly may be a real characteristic of the model rather than an artifact of numerical simulations on finite

systems of small size.

Our results for the specific heat for the various system sizes are presented in Figure 3.4, in which the curve indeed appears to stabilize for $L > 256$. The position of the peak is shown in the inset of Figure 3.4, which, within the statistical uncertainties of our calculation, is independent of system size. Our best estimate of the peak position is $T_P = 1.043(4) = 1.167(1)\ T_c$. The height of the peak is approximately 1.45. Overall, our simulations, which quantify the specific heat anomaly on lattices significantly larger than those in previous studies, have found that the peak occurs at a slightly higher temperature and is slightly shorter in height. However, the existence of the anomaly, its general shape, the fact that it stays broad (i.e., it doesn't become a cusp in the thermodynamic limit), and the fact that it occurs at a different temperature than the superfluid transition, can all be considered well-established at this point. It is worth noting that the presence of such an anomaly has been theoretically predicted by different methods, and the results of these predictions agree quantitatively with those of Monte Carlo simulations [68].

3.4 Conclusions

To summarize, we have performed extensive Monte Carlo simulations of the 2D x-y model using the Worm Algorithm. The main goals of our study were to evaluate the effectiveness of the methodology and to confirm existing theoretical results for the specific heat. We simulated the model on lattices with a linear size up to $L = 4096$, and obtained results for the superfluid transition temperature that are as accurate as those from the most recent numerical simulations, using standard computational resources. For the specific heat, the largest system size for which we report results is 16 times greater than that for which Monte Carlo estimates have been published. Our results confirm the existence of an anomaly in the specific heat, specifically a peak, that occurs at a temperature around $\sim 17\%$ higher than the superfluid transition temperature. It is interesting to compare this to 2D ^{4}He, for which computer

simulations [21] have shown that the peak in the specific heat is located at $T \sim 1.6\, T_c$.

It has been suggested [55, 69, 70] that the temperature dependence of the specific heat is related to that of the vortex density above the critical temperature. If this is the case, one might expect to see a similar specific heat anomaly in physical systems such as atomically thin ^{4}He films, which are close to the 2D limit and exhibit superfluid transitions that conform to the KT paradigm. This anomaly would not be a sign of a phase transition. This may also assist in interpreting specific heat data for ^{4}He films adsorbed on graphite, where similar features (peaks) are often taken as evidence of phase transitions (e.g., melting of commensurate solid phases, as seen in Ref. [62]).

Chapter 4

Uniaxial modulation and the Berezinskii-Kosterlitz-Thouless transition

In this chapter, we discuss our work on the superfluid transition of the classical $|\psi|^4$ field theory in 2D, while an external potential is applied in just one direction [71].

4.1 Introduction

The behavior of a quantum fluid in low dimensions is still an attractive topic of ongoing research, particularly due to recent experimental advances that enable the investigation of substances such as superfluid helium films and cold atom assemblies in novel, yet unexplored settings. In three dimensions (3D), a Bose fluid exhibits the superfluid transition at the critical temperature T_c, as well as the onset of Bose-Einstein condensation, characterized by the emergence of off-diagonal long range order (ODLRO) [5, 72].

By contrast, the two-dimensional (2D) superfluid phase does not show true ODLRO at any finite temperature, instead it presents a slow (power law) decay of spatial correlations. In this case, the superfluid transition is featured by the so-called "universal jump" of the superfluid fraction $\rho_s(T)$ as a function of temperature, from zero to a finite value as T_c is approached from above [63, 73, 74]. The theory behind the superfluid transition in 2D is explained by the Berezinskii-Kosterlitz-Thouless (BKT)

general framework [7, 13, 14].

A different approach is needed when the system is limited to just one dimension (1D), for in that case, the Tomonaga-Luttinger liquid (TLL) theory can fully explain the behavior of its low-lying excitations and its ensuing thermodynamic properties [17]. Strictly speaking, a 1D system does not have a true superfluid phase in the thermodynamic limit (i.e., $L \to \infty$, L being the system size), however, the concept of "superfluidity" can still be applied to a 1D system as a well understood and characterized finite-size effect, i.e., $\rho_s(L, T)$ is a universal function of LT [17, 75, 76]. It is important to keep in mind that while in principle, it is impossible to sustain a superfluid current (i.e., indefinitely long-lived) in 1D, the physical mechanism that leads to current decay in 1D, namely phase slips [9, 77–80], can be strongly suppressed at low temperature, to the point where a current-carrying state in 1D and a 3D superfluid have no practical experimental difference [81]. Moreover, there exist theoretical scenarios where a network of interconnected quasi-1D channels could form a 3D superflow [82, 83].

The existence of the BKT transition has been verified experimentally in various physical settings, including superfluid (^{4}He) [44–47, 49, 84] and superconducting [85] thin films, Josephson junction arrays [86] and, relatively more recently, cold atom assemblies [87–90]. In an attempt to observe Luttinger liquid behavior, several experimental approaches have been carried out to confine quantum fluids such as ^{4}He in (quasi) 1D. Particularly, the most promising approach, which has been vigorously pursued, is absorbing helium gas inside elongated cavities of nanometer size diameter, such as those that exist in a variety of porous glasses [91–96], or nanoholes in Si_3N_4 membranes [97], as well as carbon nanostructures [98, 99].

The surprising degree of control achieved on a variety of relevant systems enables one to raise fundamental theoretical questions on the behavior of superfluids in low dimensions and make predictions that can be verified in actual experiments. One such question is the possibility of changing the effective dimensionality of a superfluid by

adjusting an external parameter and detecting the resulting change in the system's behavior as described by the above-mentioned, different theoretical frameworks [25]. In order to explore some of these issues, some studies have been accomplished in the context of dipolar assemblies of cold atoms or molecules, which can create 3D parallel stripes (elongated droplets in finite systems) [100, 101] whose collective behavior can imitate that of a 2D cluster crystal [102, 103].

But even if interactions among the constituent particles are isotropic, a scenario, in which a dimensional crossover may occur, can be studied by superimposing, e.g. to a quasi-2D Bose gas, an external modulating potential of variable amplitude *along a specific direction*. In this setup, which can be done using current experimental technology for cold atoms [26–28], there should be an observation of the breakdown of the system into nearly independent, quasi-1D stripes (or "tubes"), in the presence of the sufficiently large external potential. This breakdown is conceivably concomitant with a change in the physical behavior of the system, indicating an effective change of dimensionality, from 2D to 1D. This behavior would enable the imitation of quasi 1D systems with nontrivial topology such as, for instance, junctions and/or networks of 1D channels [18, 104–107], by using pertinent modulating potentials. Additionally, it would also create a tunable and controlled environment to study the physics related to the topological Kondo effect [108–114].

In order to identify such a possible dimensional crossover, we address this scenario theoretically within the framework of the classical $|\psi|^4$ lattice field theory using means of large-scale numerical (Monte Carlo) simulations. This is an ideal choice because even though this model oversimplifies the system of interest, it still includes all the physical aspects that we wish to explore, i.e., it can exhibit a BKT superfluid transition while allowing for an externally-induced density modulation, expressed through a locally varying chemical potential.

Our main finding is that *no* dimensional crossover can be established by the uniaxial external modulation for any finite value of the amplitude of the modulation. Rather,

since the system develops quasi-1D parallel stripes in the direction perpendicular to that of the modulation, it behaves very similarly to the classical anisotropic x-y model, i.e., with different coupling along the two directions. In particular, the superfluid transition temperature T_c is suppressed due to the effect of increasing the modulation amplitude, while the anisotropy of the superfluid response can be understood as a change of length scale in one of the two directions.

The remainder of this chapter is organized as follows: in Section 4.2 we describe the model of interest; in Section 4.3 we present our results, and outline our conclusions in Section 4.4.

4.2 Model

The Hamiltonian of the classical $|\psi|^4$ field theory is given by

$$H = -t \sum_{\langle \mathbf{r}\mathbf{r}' \rangle} (\psi_{\mathbf{r}} \psi^{\star}_{\mathbf{r}'} + \psi^{\star}_{\mathbf{r}} \psi_{\mathbf{r}'}) + \sum_{\mathbf{r}} \left(\frac{U}{2} n^2_{\mathbf{r}} - \mu_{\mathbf{r}} n_{\mathbf{r}} \right) \tag{4.1}$$

This Hamiltonian is considering a square lattice of $L \times L$ sites (L even), with periodic boundary conditions in both directions; $\mathbf{r} \equiv (l_x, l_y)$ is the position of a generic lattice site, with l_x, l_y integers, $1 \leq l_{x(y)} \leq L$. While the first sum just runs over all pairs of nearest-neighboring sites, the second sum runs over all sites of the lattice. $\psi_{\mathbf{r}}$ is a complex-valued field defined at site $\mathbf{r}$ and $n_{\mathbf{r}} = |\psi_{\mathbf{r}}|^2$ is the corresponding density of particles. The parameter t stands for particle-hopping energy, which is taken as the energy unit and set equal to one. The parameter U (assumed positive in this work) represents the specific energy of interaction of particles occupying the same site (also called the on-site interaction). On the other hand, $\mu_{\mathbf{r}}$ is a (site-dependent) chemical potential, which we assume of the following form

$$\mu_{\mathbf{r}} = V_0 + V_1 \cos\left(\frac{2\pi m l_y}{L} \right) \tag{4.2}$$

$\mu_{\mathbf{r}}$ indicates an external potential, which is applied along the y-direction and has amplitude V_1. m is an integer number ranging from 1 to L, and it is a factor of L,

which means that the modulation occurs over a period of $N = L/m$.

Equation (4.1) is the classical limit of the well-known Bose Hubbard model, approached when the average occupation number $\langle n_{\mathbf{r}} \rangle \gg 1$. In the absence of an external potential (i.e., with $V_1 = 0$), and with $V_0 = U$, Equation (4.1) reduces to the x-y model, in the strong-coupling (i.e., $U \to \infty$) limit. In 2D, this model exhibits a BKT superfluid transition, in which the classical helicity modulus plays the role of the superfluid response [19]. It serves as an appropriate *minimal* model to gain insight into the physics of interest here, as our goal is to find out if there is a change in the effective dimensionality of the system when the modulation amplitude reaches a certain value. Such a change should be reflected in the critical properties of the system, which in turn reveal how it behaves over long distances, without being affected by whether the underlying field theory is formulated in the continuum or on a lattice, or whether it is quantum or classical in character.

4.3 Results

In this work, we study the possibility of a dimensional crossover in the strongly modulated $|\psi|^4$ model for different values of the modulation amplitude V_1 (4.2), in which the strongly-interacting limit is consistently recovered by setting the parameters in Equations (4.1) and (4.2) $U = V_0 = 40$, and $t = 1$ is used as the reference energy scale. Apparently, in the absence of modulation ($V_1 = 0$), this choice of parameters allows the $|\psi|^4$ model to map onto the isotropic, planar $x - y$ model with uniform coupling parameter J [115]; since the $x - y$ model is a limiting case of the $|\psi|^4$ theory, approached when $U = c \to \infty$. In this setting, multiple occupation of the same site is physically penalized by the repulsive interaction among particles. Without reducing generality, we select the modulation period $N = 8$ for every studied value of V_1.

In order to validate whether our model can describe the system of interest or not, we map out the density map of the simulated system for a large amplitude of the modulation $V_1 = 80$ at low temperature. As expected, the reliability of our model

is confirmed, the system breaks down into stripes for sufficiently large values of the amplitude of the modulating potential, wherein the energy barrier needed for multiple occupation is overcome (as shown in Figure 4.1).

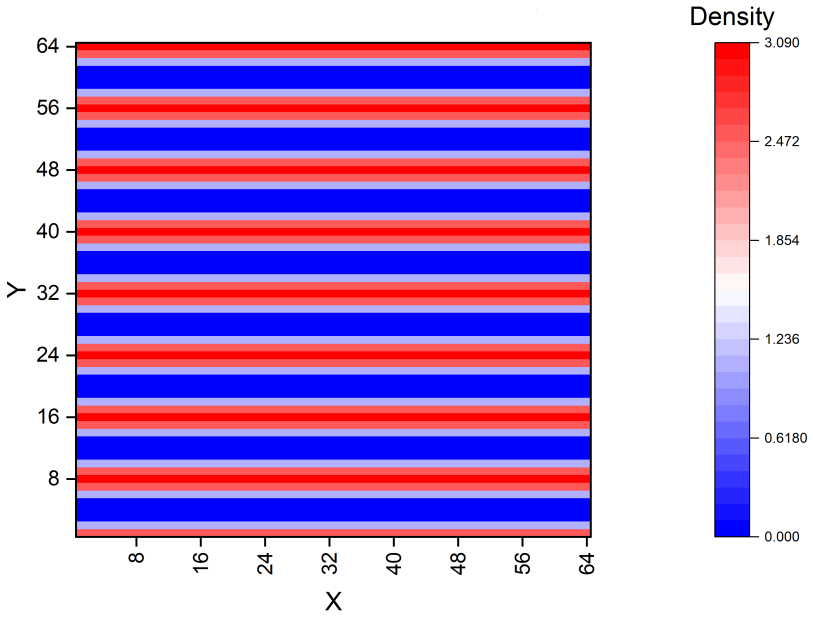

Figure 4.1: Density map at low temperature of the system represented by the 2D $|\psi|^4$ classical Hamiltonian in the presence of an external modulation. The formation of stripes is evident.

To exploit the effect of a large modulating potential, we illustrate our estimates for the superfluid fraction along each direction as a function of temperature for the various lattice sizes considered $L = 64, 128, 256, 512, 1024$, and for two different values of the modulation amplitude $V_1 = 40$ and $V_1 = 60$.

In the upper (lower) panel of Figure 4.2, we plot the superfluid fraction along the x-direction (the y-direction) $\rho_{S,x(y)}(T, L)$ for $V_1 = 40$ as a function of T for increasing values of L. Similar to the case of the isotropic, planar $x - y$ model (discussed in Chapter 3), as L increases, both $\rho_{s,x}(T, L)$ and $\rho_{s,y}(T, L)$ become sharper, and move closer to the vertical red line, which indicates the trend of the superfluid fraction in the thermodynamic limit, following the BKT formalism. Apparently, on increasing L, both $\rho_{s,x}(T, L)$ and $\rho_{s,y}(T, L)$ get shaped so to exhibit the universal jump at $T = T_c$, although $\rho_{s,y}(T_c)$ is rescaled with respect to $\rho_{s,x}(T_c)$.

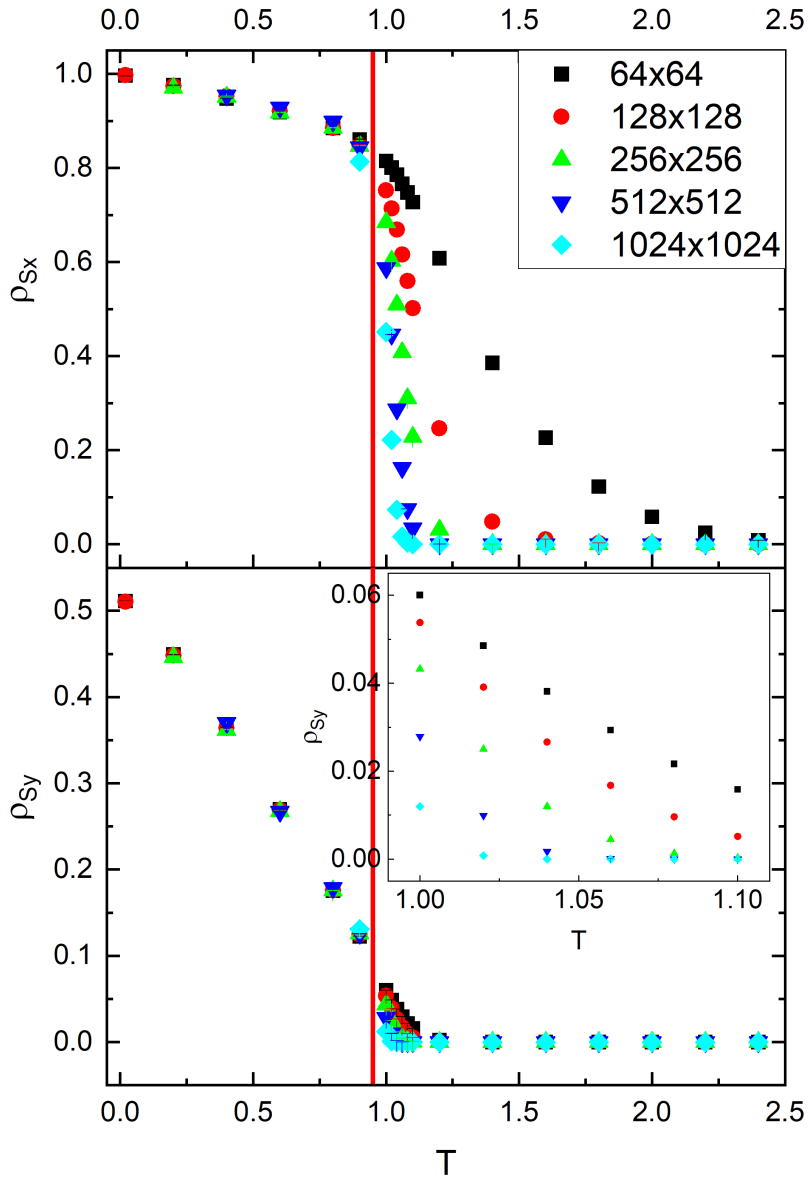

Figure 4.2: *Upper panel:* The superfluid fraction along the x-direction (longitudinal) ρ_{Sx} versus temperature, for the different lattice sizes considered, with the modulation strength $V_1/t = 40$. Statistical errors are smaller than symbol sizes. The vertical red line indicates the critical temperature. *Lower panel:* Same as Upper panel for the y-direction (transverse).

In Figure 4.3, we present plots similar to the ones in Fig. 4.2, but now for $V_1 = 60$. In this case, the superfluid response along the y-direction is suppressed, and for large modulation becomes negligible except at a very low temperature. Thus, one can argue that the superfluid response along the y-direction totally vanishes, its small finite

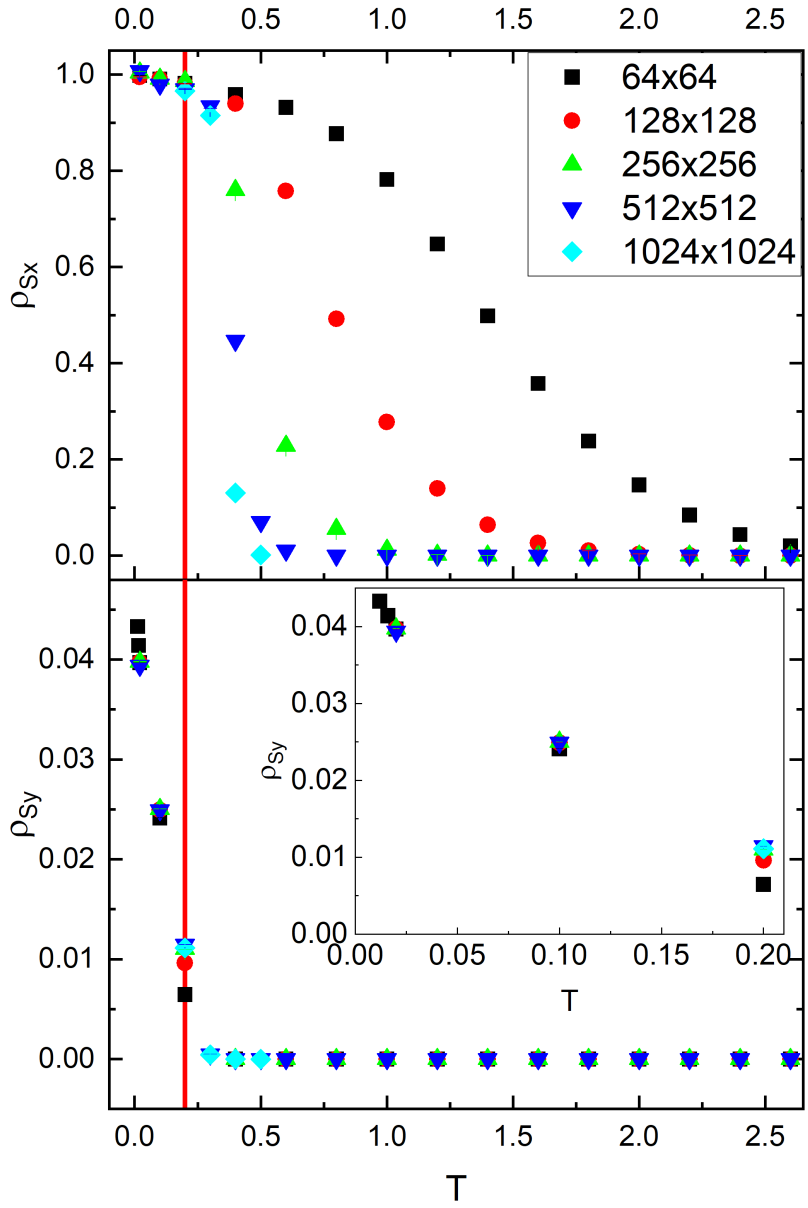

Figure 4.3: Same as Figure 4.2 for the modulation strength $V_1/t = 60$.

value at the sufficiently low temperature is just a finite-size effect, and the dimensional crossover actually occurs in this case. Aware of this argument, as shown in Figure 4.3, we have carried out a finite-size scaling analysis of our results, showing that this small finite value of the superfluid fraction along the y-direction stays unchanged when increasing the lattice size. In other words, this is not a finite-size effect, and this small finite value survives in the thermodynamic limit. Overall, the behavior of $\rho_{s,x}(T)$ and

$\rho_{s,y}(T)$ is exactly the same as for $V_1 = 40$, however, increasing V_1 has decreased the value of T_c and significantly reduced $\rho_{s,y}(T, L)$ in comparison to $\rho_{s,x}(T, L)$, which is consistent with Figure 4.2. Despite this, $\rho_{s,y}(T, L)$ still bends towards the finite universal jump at $T = T_c$, as it is appropriate for the two-dimensional system.

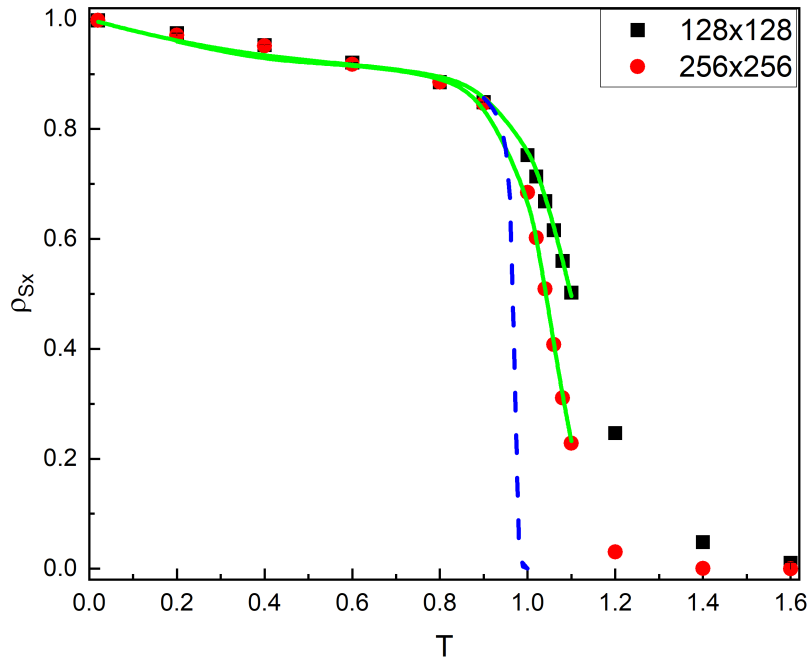

Figure 4.4: The superfluid fraction along the x-direction ρ_{Sx} as a function of temperature, for the two different lattice sizes, with the modulation strength $V_1/t = 40$. Boxes and circles are numerical estimates obtained by Monte Carlo simulations. Solid lines are fits to the data based on the BKT recursive equations (see text), while dashed line represents the extrapolation to the thermodynamic limit.

In order to verify that our studied system always falls in the BKT universality class, we carry out a fit to our numerical estimates for the superfluid fraction along the x-direction ρ_{Sx} for $V_1/t = 40$ using the modified BKT recursive equations applying for the classical anisotropic $x - y$ model [71] (as shown in Figure 4.4). One can see that the fit displays an impressive quality for both the two different lattice sizes considered, especially in the vicinity of the critical temperature T_c. Based on the fit to the data for our finite system, the behavior of the superfluid fraction in the thermodynamic limit can be extrapolated, and indicated by the dashed curve in Figure 4.4; and with the help of the well-known universal jump condition [63], we estimate the superfluid

transition temperature $T_c = 0.95(5)$.

Our results clearly show that no dimensional crossover can be caused by the uniaxial external potential modulation for any finite value of the amplitude of the modulation: the only effects of increasing V_1 are a combined suppression of the critical temperature T_c and of the ratio between $\rho_{s,y}(T)$ and $\rho_{s,x}(T)$, without qualitatively affecting the behavior of the system. A finite, though small, superfluid fraction always appears at $T \to 0$ in both directions, as well as a finite, though small, T_c at which the system undergoes the BKT phase transition.

4.4 Conclusions

In this work, we explored how a uniaxial external modulation affects a two-dimensional superfluid. The behavior of the superfluid at a finite temperature was studied using the classical $|\psi|^4$ model on a square lattice. By incorporating the modulation into the well-established mapping between the $|\psi|^4$ and the $x - y$ model, a version of the latter model Hamiltonian with modulated parameters was developed. This enables the examination of the effects of progressively increasing the potential modulation strength V_1.

We demonstrated that even though the system tends to form quasi 1D stripes perpendicular to the direction of the modulation, the classical anisotropic $x-y$ model still accurately depicts the superfluid phase transition at any value of V_1. This is because the modulated model simplifies to the classical anisotropic $x - y$ model in the large-scale, low-energy limit. In particular, we have shown that the primary effects of increasing V_1 are causing T_c to decrease to a finite value and also lowers the ratio between the superfluid fractions at $T \to 0$, $\rho_{s,y}(0)/\rho_{s,x}(0)$. As a result, as long as the systems being studied are large enough, a relevant measurement of the superfluid fractions always evidences the two-dimensionality of the superfluid [116–118].

Because our minimal model can be widely used to illustrate the superfluid phase transition in planar, interacting bosonic systems, we conclude that, as a general re-

sult, simply applying a uniaxial modulation is not sufficient to induce a 2D to 1D dimensional crossover in such systems.

Additional ways to approach our research could include, but are not limited to, looking at how disorder affects the sample. It would be intriguing to determine if the scenario we observed is influenced by impurities. Given the high level of control achieved in cold atom technology, it may be possible to create impurities with tunable parameters, mimicking junctions of quantum wires [119–124], or even network of junctions [125], with high level of quantum coherence [126, 127] and a wide range of potential practical applications.

Chapter 5

Phase diagram of hard core bosons with anisotropic interactions

In this chapter, we discuss our results of an examination of the phase diagram of a system of hard core bosons on the square lattice, where the bosons interact with each other through an anisotropic potential that only affects their nearest neighbors [39].

5.1 Introduction

Lattice hard core bosons have been a subject of theoretical study for a long time, due to their use as a minimal model for a system with strong interactions that shows a superfluid phase at low temperatures and a quantum phase transition between superfluid and crystalline ground states. Moreover, the investigation of this model has provided a lot of understanding about the possibility of a supersolid phase, and how defects such as vacancies and interstitials may be involved in its stability [30–38].

For a long time, lattice models were considered to be of little practical use and only of interest to academics, as they were unable to provide a realistic microscopic description of any actual physical system. However, in recent years, advancements in optical lattice technology have made it possible to create artificial many-body systems using ultracold atoms and molecules, which can accurately simulate the physics outlined in lattice models [128–132]. Therefore, with the use of artificial many-body systems, one can now compare theoretical predictions and experimental results with

a high degree of precision, which is not possible with naturally occurring physical systems such as solid helium. Additionally, the possibility of engineering interactions among cold atoms [133–137] not occurring in ordinary condensed matter (at least not as the dominant interactions) could open the door to the discovery of novel, exotic phases of matter [102, 138, 139].

For instance, recent developments in experimental techniques in the spatial confinement and cooling of large assemblies of atoms with finite electric and magnetic dipoles, enable the study of many-body systems whose interaction is *primarily* dipolar, i.e., anisotropic (attractive or repulsive depending on the relative direction of approach of two particles). These interactions may not be strictly long-ranged, but they can still extend to distances significantly beyond nearest neighbors, at experimentally attainable densities. It is believed that different crystalline and/or superfluid phases, breaking rotational symmetry in principle can be stabilized by these two features of the pairwise interaction.

There have been a lot of studies, both through experimentation [140] and theory [141, 142], of the physics of a system made up of spin zero particles possessing a dipole moment, with all dipole moments aligned along the same direction. In three dimensions, computer simulations of continuous systems have observed a supersolid phase [103, 143]. Two-dimensional systems are more intricate; possible supersolid phases that were thought to happen in speculated "microemulsion" scenarios, where the dipole moments are perpendicular to the plane of particle movement [144], have been proven to not exist [145]. On the other hand, computer simulations have shown the existence of supersolid phases in dipolar bosons on a triangular lattice [146], whereas it has been confirmed that such phases cannot be stabilized on a square lattice [147], even if dipole moments are tilted with respect to the direction perpendicular to the plane of particle motion, a prediction confirmed for continuous systems [148][1].

[1]When the tilting angle exceeds a critical value in three dimensions or lower dimensions, the interaction between dipoles becomes purely attractive in specific directions, causing the system to become unstable and collapse. To prevent this, a short-range hard core repulsion must be supple-

An interesting question that can be explored theoretically is how the long-range nature of the interaction affects the stability of specific, exotic thermodynamic phases, e.g., the supersolid. As an example, the phase diagram of lattice dipolar bosons of spin zero, with dipole moments aligned perpendicularly to the plane of motion, is qualitatively similar to that with only nearest-neighbor interactions, both on the square [33, 147] and on the triangular lattice [38, 146]. In particular, there are interstitial supersolid phases on the triangular lattice, at particle density 1/3 (2/3), while no supersolid phase is found at half filling on the square one. Remarkably, by including *only* nearest and next-nearest neighbor interactions, it is possible to stabilize vacancy and interstitial supersolid phases on the square lattice at density 1/4 (3/4) [149, 150].

In this chapter, we present the findings of a theoretical examination of the phase diagram of a system of hard core bosons on the square lattice, interacting via an anisotropic nearest-neighbor potential, with the repulsive interaction in one direction and the attractive interaction in the other. We map out the complete finite temperature phase diagram, which is found to be qualitatively very similar to that of a system of hard-core dipolar bosons with aligned dipole moments, tilted with respect to the perpendicular to the plane. The interplay of attraction and repulsion along different directions results in the existence of three distinct phases: a superfluid (SF) one, as well as two crystalline phases at half filling, specifically a checkerboard (CB) and a striped (ST) phase. There is no detection of a supersolid phase, even at exactly half filling, which is in line with fundamental theoretical explanations [151], or by doping either the CB or ST phase with vacancies or interstitials. Each crystalline phase is separated from the superfluid by a conventional first order quantum phase transition at zero temperature. The fundamental characteristics of the finite temperature phase diagram are also in agreement with what is observed in other models of lattice

mented to the dipolar interaction, whose presence is customarily assumed in standard theoretical studies, to ensure thermodynamic stability.

hard-core bosons.

The remainder of this chapter is organized as follows: in Section 5.2 we describe the model of interest; in Section 5.3 we present our results, and outline our conclusions in Section 5.4.

5.2 Model

We are interested in the well-known lattice hard core Bose Hamiltonian, expressed as follows:

$$\begin{aligned} \hat{H} = & - t \sum_{\mathbf{r}} \left(\hat{a}^{\dagger}_{\mathbf{r}+\hat{\mathbf{x}}} \, \hat{a}_{\mathbf{r}} + \hat{a}^{\dagger}_{\mathbf{r}+\hat{\mathbf{y}}} \, \hat{a}_{\mathbf{r}} + h.c. \right) + \\ & + \sum_{\mathbf{r}} \left(V_{\mathbf{r},\hat{\mathbf{x}}} \, \hat{n}_{\mathbf{r}} \, \hat{n}_{\mathbf{r}+\hat{\mathbf{x}}} + V_{\mathbf{r},\hat{\mathbf{y}}} \, \hat{n}_{\mathbf{r}} \, \hat{n}_{\mathbf{r}+\hat{\mathbf{y}}} \right) + \\ & - \mu \sum_{\mathbf{r}} \hat{n}_{\mathbf{r}}, \end{aligned} \tag{5.1}$$

where the sum runs over all the sites of a square lattice of $N = L \times L$ sites, with periodic boundary conditions. Here, $\hat{\mathbf{x}}$ and $\hat{\mathbf{y}}$ are the unit vectors in the two crystallographic directions, $\hat{a}^{\dagger}_{\mathbf{r}}$, $\hat{a}_{\mathbf{r}}$ are the standard Bose creation and annihilation operators, $n_{\mathbf{r}} \equiv \hat{a}^{\dagger}_{\mathbf{r}} \, \hat{a}_{\mathbf{r}}$ is the occupation number for site $\mathbf{r}$, t is the particle-hopping matrix element and μ is the chemical potential. Particularly, there is the definition of the (nearest-neighbor) interaction potential:

$$V_{\mathbf{r},\hat{\mathbf{x}}} = V, \quad V_{\mathbf{r},\hat{\mathbf{y}}} = \lambda \, V, \tag{5.2}$$

λ being a real number. The Hamiltonian (5.1) is defined in the subspace of many-particle configurations, where no more than one particle can occupy a single lattice site, known as the hard core condition. Therefore, the total number of particles $N_P \equiv \sum_{\mathbf{r}} \hat{a}^{\dagger}_{\mathbf{r}} \hat{a}_{\mathbf{r}}$ can take on any integer value from 0 to N. The particle density (or, filling) is defined as $\rho \equiv (N_P/N)$, i.e., $0 \leq \rho \leq 1$.

In this model, the phase diagram of the isotropic $\lambda = 1$ case has been extensively studied; it is known that, for $-2t < V < 2t$, the system exhibits a single homogeneous

fluid phase, undergoing a SF transition at low temperature. Besides, if $V > 2t$ there is a first order quantum phase transition appearing at temperature $T = 0$ between a SF and a CB crystal at half filling (i.e., $\rho = 1/2$) [33]. For $V < -2t$, only two phases exist, characterized by either $\rho = 0$ or 1, phases of intermediate filling (some of them SF) can only be stabilized by external factors, such as disorder [152].

On the other hand, the $\lambda \neq 1$ case has not been extensively studied, primarily due to the difficulty in finding a practical way to conduct experiments for this case. However, an interaction with that kind of anisotropy can be achieved in dipolar systems by simply adjusting the alignment of dipole moments with respect to the direction perpendicular to the plane of the lattice (see, for instance, Ref. [147] for details). While the dipolar interaction extends significantly beyond nearest neighboring lattice sites, in this work we aim to determine which characteristics of the phase diagram are solely due to the anisotropy in the short-range portion of the interaction. Of particular interest is the case $\lambda < 0$, i.e., the interaction is repulsive (attractive) in the x (y) direction.

In this work, we systematically investigated the finite temperature phase diagram of Eq. 5.1, as a function of the three parameters T, μ and λ. In order to characterize the various phases of the system we computed the superfluid density $\rho_S(T)$ using the well-known winding number estimator [153], as well as the static structure factor

$$S(\mathbf{Q}) = \frac{1}{N^2} \left\langle \left| \sum_{\mathbf{r}} \hat{n}_{\mathbf{r}} \; e^{i\mathbf{Q}\cdot\mathbf{r}} \right|^2 \right\rangle \tag{5.3}$$

where $\langle ... \rangle$ stands for thermal average. A finite value of $S(\mathbf{Q})$ for some specific wave vector(s) signals the presence of crystalline long-range order. In particular, the wave vector $\mathbf{Q} = (\pi, \pi)$ is related to checkerboard order, while $\mathbf{Q} = (\pi, 0)$ (and not $(0, \pi)$ because of the way we have defined the interaction, Equation (5.2)) indicates stripe order, in both cases at half filling. Numerical simulations have been carried out on square lattices of different sizes (up to $L = 32$) in order to evaluate the impact of finite size effects.

5.3 Results

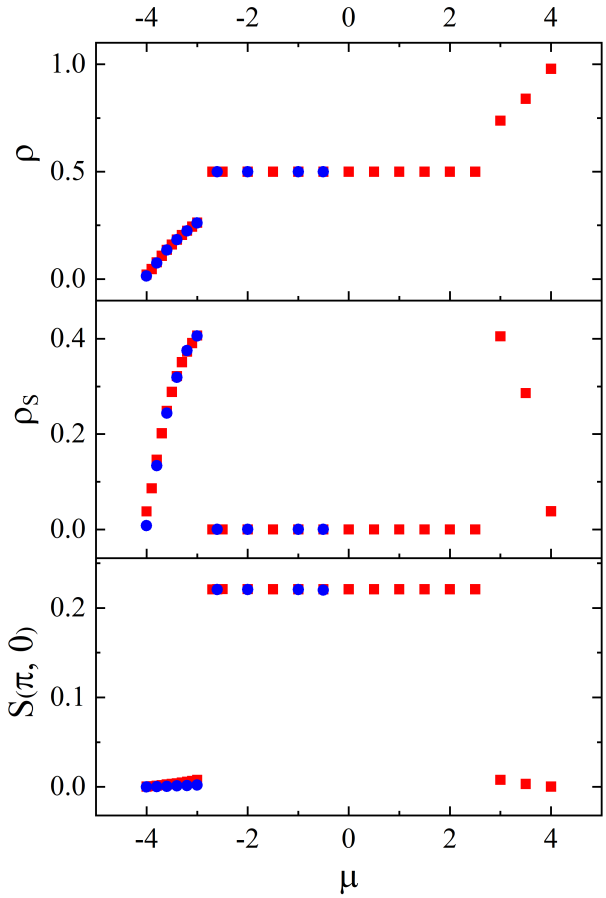

Figure 5.1: Ground state particle density ρ (top panel), superfluid density ρ_S (middle panel) and static structure factor $S(\pi, 0)$ (bottom panel) versus chemical potential μ (in units of t) for $V/t = 3$, $\lambda = -1$ and two system sizes $L = 8$ (boxes), $L = 16$ (circles). Statistical errors are smaller than symbol sizes.

We begin by discussing the physical behavior of the system in its ground state, i.e., at temperature $T = 0$. Since we use a simulation method that takes into account a finite temperature, we can achieve our goal by extrapolating to the $T = 0$ limit results obtained at sufficiently low temperatures. In practice, our numerical estimates are computed at temperature $T \sim T_L \equiv (t/L)$, which are indistinguishable from the extrapolated ones, within the statistical uncertainties of the calculation. This means that the physical estimates obtained at T_L can be considered to be equivalent to those obtained in the ground state.

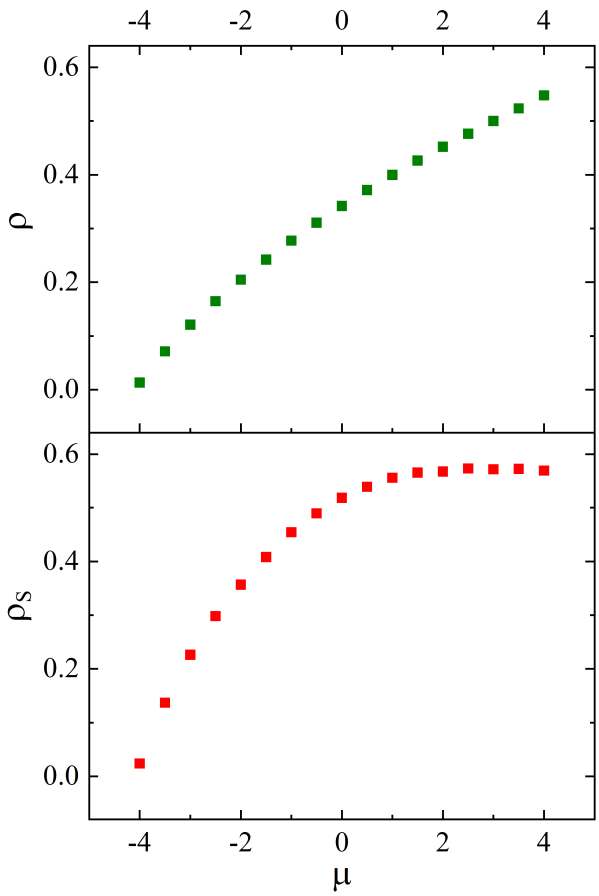

Figure 5.2: Same as Figure 5.1 for $\lambda = 0$.

An example of how the phases of the system are identified is shown in Figure 5.1, which shows ground state results for the case $\lambda = -1$ and $V = 3t$. In this case, the system presents two distinct phases, a superfluid one (possessing no crystalline order) away from half filling, and a non-superfluid crystalline (striped) one at half filling. These two phases are separated by a first order phase transition.

Specifically, the top panel displays the dependence of the computed particle density ρ on the chemical potential μ (in units of t). The density jump as ρ approaches half filling indicates a first-order phase transition, with coexistence of a superfluid phase (expressed through the superfluid density ρ_S in the middle panel), and one that features striped crystalline order (expressed through the static structure factor $S(\pi, 0)$ in the bottom panel). As one can see, no supersolid phase exists, i.e., in which

both ρ_S and $S(\pi, 0)$ are finite. The superfluid density is finite throughout the system, except at half filling, while the static structure factor is finite only at half filling. This can be contrasted with the results shown in Figure 5.2 for $V/t = 3$ and $\lambda = 0$. In this case, all the curves are smooth throughout, indicating that there is no phase transition.

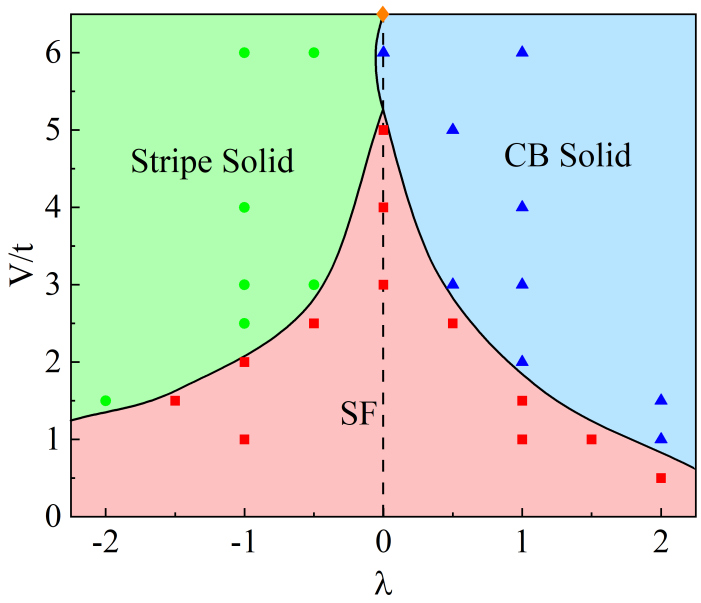

Figure 5.3: Ground state phase diagram at half filling as a function of the interaction strength V and anisotropy parameter λ. The system features a checkerboard solid (triangles), a stripe solid (circles), and a superfluid phase (boxes). In the $V/t \to \infty$ limit, the CB solid and the stripe solid lines meet at $\lambda = 0$ (diamond at the top). Solid lines separating the various phases indicate first order quantum phase transitions.

Based on the analysis of the results such as those shown in Figure 5.1 and Figure 5.2, the ground state phase diagram at half filling in the $V - \lambda$ plane is shown in Figure 5.3. This illustrates the boundaries between the three different phases that are observed, namely the SF as well as CB and striped solid phases. Lines that separate the different phases depict first-order quantum phase transitions. This phase diagram is qualitatively very similar to that of a system of tilted dipolar lattice bosons [147]. As expected, at low interaction strength V (the weak coupling limit) the system displays the SF phase for any value of the anisotropic parameter λ. On the other hand,

as V is increased to a critical value $V_c(\lambda)$ the system undergoes a first-order phase transition and changes into a checkerboard (striped) solid phase when $\lambda > 0$ ($\lambda < 0$). As $\lambda \to 0$, the system remains in a superfluid state even at higher values of the interaction strength V. However, for $V \gtrsim 5t$, the system can only exist in one of the two crystalline phases.

Along the $\lambda = 0$ line, quantum fluctuations make the CB phase more favorable than the striped one, which can be confirmed by using standard second order perturbation theory. Therefore, the boundary line between the stripe phase and the CB phase at large values of V is not exactly vertical, as CB order is favored for $\lambda \to 0^-$. This is seemingly the most significant contrast between the anisotropic nearest-neighbor interaction studied in this work and the tilted, full dipolar interaction [147].

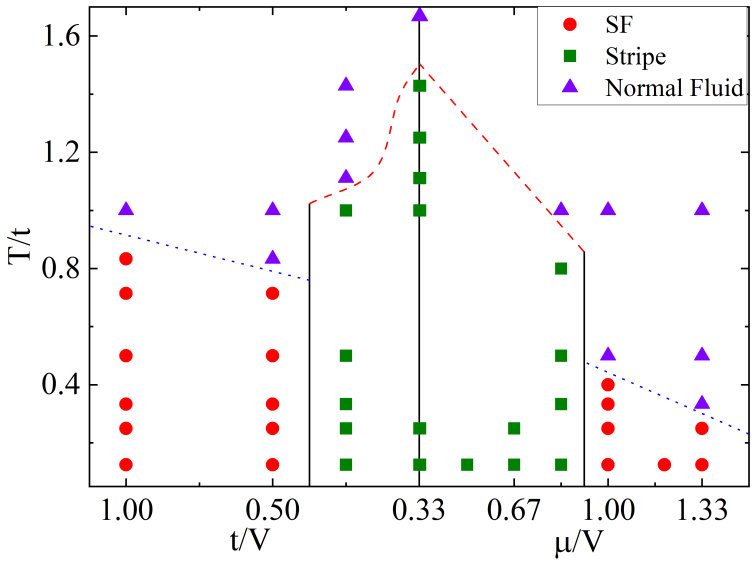

Figure 5.4: Finite temperature phase diagram for $\lambda = -1$ for two representative cuts. Left panel show results for fixed $\mu = t$; the right panel is for fixed $V = 3\ t$. Solid lines indicate first-order phase transitions between stripe solid (boxes) and superfluid (circles) or normal fluid (triangles) phases. Dotted lines show Berezinskii-Kosterlitz-Thouless transitions between normal fluid (triangles) and superfluid phases. Dashed lines correspond to second-order transitions in the Ising universality class between stripe solid and normal fluid.

The finite-temperature phase diagram of the system in the (T, μ, V) space is presented in Figure 5.4 with two representative cuts. We consider for definiteness the

case $\lambda = -1$, for which the ground state at half filling is a stripe solid for $V \gtrsim 2.5\ t$. The panel on the left displays a constant chemical potential ($\mu = t$), while the panel on the right displays a constant interaction strength ($V = 3\ t$).

At constant temperature, a first-order (quantum) phase transition separates the striped crystal from the (super)fluid phase in Figure 5.4. On the other hand, at constant V or μ superfluid order is destroyed by thermal fluctuations and turns into a normal fluid through a Berezinskii-Kosterlitz-Thouless transition, indicated by the dotted lines. Additionally, the striped crystal melts into a normal fluid via a second-order transition in the Ising universality class, shown by the dashed curve in Figure 5.4. Overall, this phase diagram is fairly conventional, and qualitatively identical to that in the $\lambda > 0$ sector, with no supersolid phase.

All of the phase boundaries drawn in Figure 5.3 and Figure 5.4 are only qualitatively sketched.

5.4 Conclusions

In this work, we examine the phase diagram of a system of hard core bosons on the square lattice, where the interaction between bosons is a short-ranged (nearest-neighbor) interaction and can differ in the two crystallographic directions. This includes the situation where the bosons are attracted in one direction but repelled in another. One can realize this kind of anisotropic interaction experimentally with a system of dipolar atoms or molecules, confined to a 2D optical lattice, if dipole moments are adjusted at a varying (tilting) angle with respect to the direction perpendicular to the plane of particle motion.

The purpose of this study are *a*) to comprehend the different phases that can emerge due to the anisotropy of the interaction, *b*) to evaluate the significance of its extended range, by comparing our results to those obtained in similar studies [147] that take into account the full dipolar interaction. With respect to the case in which the interaction is isotropic, the only variation observed is the emergence

of a distinct crystalline phase with stripe order. Otherwise, the phase diagram is qualitatively identical to that for isotropic interaction, featuring a single crystalline phase at half filling, and no supersolid phase. The phase diagram is also qualitatively identical to that observed by considering the full dipolar interaction, i.e., extending beyond nearest neighbors, with different degrees of anisotropy matching different tilting angles [147]. This is in agreement with what has been seen in the case of purely repulsive, isotropic interactions, where the existence of a $1/r^3$ dipolar tail does not significantly change the phase diagram, e.g., on the triangular lattice [146]. Overall, this study supports the idea that lattice geometry (i.e., triangular versus square) has a greater impact on the emergence of supersolid phases than the detailed form of the interaction.

According to a recent study [154], it has been proposed that supersolid phases can be stabilized in the presence of anisotropic dipolar interactions extending to next-nearest neighboring distances. This aspect is not explored here, but the contention seems plausible and not particularly surprising, since this was expressed to be the case for isotropic repulsive interactions [150] (i.e., the $\lambda > 0$ sector of Eq. 5.2), and the fact that the system in the positive λ sector behaves qualitatively similar to that in the negative λ sector, as shown in this work.

Chapter 6

Conclusions

We have investigated some aspects of the superfluid transition in low dimensions and/or in the presence of external modulating fields, making use of classical and quantum lattice models. Driving this investigation is recent advancements in technology, which allow for the exploration of, e.g., superfluid helium films or cold atom assemblies in novel, yet unexplored settings. These studies have been carried out by means of new computational methods, such as the Worm Algorithm in the lattice flow representation, which has the ability to provide quantitative predictions valid in the thermodynamic limit.

First, we have studied the behavior of the specific heat in a 2D superfluid by performing large-scale numerical simulations of the 2D classical x-y model, which falls in the same universality class (BKT) as quasi-2D superfluid ^{4}He films. This behavior of the specific heat is still poorly understood due to an unclear anomaly appearing above the superfluid transition temperature in 2D, while there is a sharp peak related to the superfluid transition in 3D. Our results justify the presence of a specific heat anomaly, which remains a rounded anomaly, and locates at a temperature $\sim 17\%$ higher than the superfluid transition temperature. Specifically, this is not indicative of a phase transition.

Second, we have explored whether a dimensional crossover in a 2D superfluid can be induced by the effects of a strong external modulating potential, applying to the

system in just one direction, in the context of the classical $|\psi|^4$ field theory. This model can exhibit a BKT phase transition, and is a generalization of the x-y model in which the local density of the system can vary. We have found that, if the studied systems are large enough, the two-dimensionality of the superfluid is always evidenced by a pertinent measurement of the superfluid fractions. Overall, despite the tendency of the system to form quasi 1D stripes perpendicular to the direction of the modulation, for any finite value of the modulation amplitude, the physics of the system approaches that of the anisotropic $x-y$ model, with a suppressed superfluid transition temperature and an anisotropic response, but with no dimensional crossover.

Finally, we have investigated the phase diagram of a system of hard-core bosons on the square lattice, that interacts through an anisotropic nearest-neighbor potential, in which the interaction is repulsive in one direction and attractive in another. This ground state phase diagram consists of three distinguished phases: a superfluid phase, as well as two crystalline phases (checkerboard or striped) at half-filling, but no "supersolid" phase; which is similar to the scenario of isotropic interactions. Moreover, a complete finite temperature phase diagram is also mapped out, and the behavior of this is qualitatively very similar to that of a system of hard-core dipolar bosons with aligned dipole moments, tilted with respect to the perpendicular to the plane. The main results that should be highlighted are this model contains no supersolid phase, and long-range interactions do not result in significant new physics compared to what can be observed in a system with short-range interactions only.

Bibliography

[1] P. Kapitza, "Viscosity of liquid helium below the λ-point," *Nature*, vol. 141, no. 3558, pp. 74–74, Jan. 1938, ISSN: 1476-4687. DOI: 10.1038/141074a0. [Online]. Available: https://doi.org/10.1038/141074a0.

[2] J. F. ALLEN and A. D. MISENER, "Flow of liquid helium ii," *Nature*, vol. 141, no. 3558, pp. 75–75, Jan. 1938, ISSN: 1476-4687. DOI: 10.1038/141075a0. [Online]. Available: https://doi.org/10.1038/141075a0.

[3] L. TISZA, "Transport phenomena in helium ii," *Nature*, vol. 141, no. 3577, pp. 913–913, May 1938, ISSN: 1476-4687. DOI: 10.1038/141913a0. [Online]. Available: https://doi.org/10.1038/141913a0.

[4] A. J. Leggett, "Can a solid be "superfluid"?" *Phys. Rev. Lett.*, vol. 25, pp. 1543–1546, 22 Nov. 1970. DOI: 10.1103/PhysRevLett.25.1543. [Online]. Available: https://link.aps.org/doi/10.1103/PhysRevLett.25.1543.

[5] A. J. Leggett, *Quantum Liquids: Bose condensation and Cooper pairing in condensed-matter systems*. Oxford University Press, Sep. 2006, ISBN: 9780198526438. DOI: 10.1093/acprof:oso/9780198526438.001.0001. [Online]. Available: https://doi.org/10.1093/acprof:oso/9780198526438.001.0001.

[6] D. R. Tilley and J. Tilley, *Superfluidity and Superconductivity*. Routledge, 1990. DOI: 10.1201/9780203737897. [Online]. Available: https://doi.org/10.1201/9780203737897.

[7] J. M. Kosterlitz and D. J. Thouless, "Ordering, metastability and phase transitions in two-dimensional systems," *Journal of Physics C: Solid State Physics*, vol. 6, no. 7, p. 1181, 1973. DOI: 10.1088/0022-3719/6/7/010.

[8] R. J. Glauber, "Coherent and incoherent states of the radiation field," *Phys. Rev.*, vol. 131, pp. 2766–2788, 6 Sep. 1963. DOI: 10.1103/PhysRev.131.2766. [Online]. Available: https://link.aps.org/doi/10.1103/PhysRev.131.2766.

[9] J. S. Langer, "Coherent states in the theory of superfluidity," *Phys. Rev.*, vol. 167, pp. 183–190, 1 Mar. 1968. DOI: 10.1103/PhysRev.167.183. [Online]. Available: https://link.aps.org/doi/10.1103/PhysRev.167.183.

[10] J. S. Langer, "Coherent states in the theory of superfluidity. ii. fluctuations and irreversible processes," *Phys. Rev.*, vol. 184, pp. 219–229, 1 Aug. 1969. DOI: 10.1103/PhysRev.184.219. [Online]. Available: https://link.aps.org/doi/10.1103/PhysRev.184.219.

[11] Y. Xu, W. Jäger, J. Tang, and A. R. W. McKellar, "Spectroscopic studies of quantum solvation in $^4He_N-N_2O$ clusters," *Phys. Rev. Lett.*, vol. 91, p. 163 401, 16 Oct. 2003. DOI: 10.1103/PhysRevLett.91.163401. [Online]. Available: https://link.aps.org/doi/10.1103/PhysRevLett.91.163401.

[12] N. D. Mermin and H. Wagner, "Absence of ferromagnetism or antiferromagnetism in one- or two-dimensional isotropic heisenberg models," *Phys. Rev. Lett.*, vol. 17, pp. 1133–1136, 22 Nov. 1966. DOI: 10.1103/PhysRevLett.17.1133. [Online]. Available: https://link.aps.org/doi/10.1103/PhysRevLett.17.1133.

[13] V. L. Berezinskii, "Destruction of long-range order in one-dimensional and two-dimensional systems possessing a continuous symmetry group. ii. quantum systems," *Sov. Phys. JETP*, vol. 34, no. 3, pp. 610–616, 1972.

[14] J. M. Kosterlitz and D. J. Thouless, "Long range order and metastability in two dimensional solids and superfluids. (application of dislocation theory)," *Journal of Physics C: Solid State Physics*, vol. 5, no. 11, p. L124, 1972. DOI: 10.1088/0022-3719/5/11/002.

[15] J. M. Kosterlitz and D. J. Thouless, "The critical properties of the two-dimensional xy model," *Journal of Physics C: Solid State Physics*, vol. 7, no. 6, p. 1046, 1974. DOI: 10.1088/0022-3719/7/6/005.

[16] D. R. Nelson, "Xvi. superfluidity and the two dimensional xy model," *Physics Reports*, vol. 49, no. 2, pp. 255–259, 1979, ISSN: 0370-1573. DOI: https://doi.org/10.1016/0370-1573(79)90116-9. [Online]. Available: https://www.sciencedirect.com/science/article/pii/0370157379901169.

[17] F. D. M. Haldane, "Effective harmonic-fluid approach to low-energy properties of one-dimensional quantum fluids," *Phys. Rev. Lett.*, vol. 47, pp. 1840–1843, 25 Dec. 1981. DOI: 10.1103/PhysRevLett.47.1840. [Online]. Available: https://link.aps.org/doi/10.1103/PhysRevLett.47.1840.

[18] T. Giamarchi, "Theoretical framework for quasi-one dimensional systems," *Chem. Rev.*, vol. 104, no. 11, pp. 5037–5056, 2004. DOI: 10.1021/cr030647c.

[19] M. E. Fisher, M. N. Barber, and D. Jasnow, "Helicity modulus, superfluidity, and scaling in isotropic systems," *Phys. Rev. A*, vol. 8, pp. 1111–1124, 2 Aug. 1973. DOI: 10.1103/PhysRevA.8.1111.

[20] N. Prokof'ev and B. Svistunov, "Worm algorithms for classical statistical models," *Physical Review Letters*, vol. 87, no. 16, p. 160 601, 2001. DOI: 10.1103/PhysRevLett.87.160601.

[21] D. M. Ceperley and E. L. Pollock, "Path-integral simulation of the superfluid transition in two-dimensional ^4He," *Phys. Rev. B*, vol. 39, pp. 2084–2093, 4 Feb. 1989. DOI: 10.1103/PhysRevB.39.2084. [Online]. Available: https://link.aps.org/doi/10.1103/PhysRevB.39.2084.

[22] R. Gupta and C. F. Baillie, "Critical behavior of the two-dimensional xy model," *Physical Review B*, vol. 45, no. 6, pp. 2883–2898, 1992. DOI: 10.1103/PhysRevB.45.2883.

[23] J. E. Van Himbergen and S. Chakravarty, "Helicity modulus and specific heat of classical XY model in two dimensions," *Phys. Rev. B*, vol. 23, pp. 359–361, 1 Jan. 1981. DOI: 10.1103/PhysRevB.23.359. [Online]. Available: https://link.aps.org/doi/10.1103/PhysRevB.23.359.

[24] P. H. Nguyen and M. Boninsegni, "Superfluid transition and specific heat of the 2d x-y model: Monte carlo simulation," *Appl. Sci.*, vol. 11, no. 11, 2021, ISSN: 2076-3417. DOI: 10.3390/app11114931.

[25] S. Lammers, I. Boettcher, and C. Wetterich, "Dimensional crossover of non-relativistic bosons," *Phys. Rev. A*, vol. 93, p. 063 631, 6 Jun. 2016. DOI: 10.1103/PhysRevA.93.063631. [Online]. Available: https://link.aps.org/doi/10.1103/PhysRevA.93.063631.

[26] T. Kinoshita, T. Wenger, and D. S. Weiss, "Observation of a one-dimensional tonks-girardeau gas," *Science*, vol. 305, no. 5687, pp. 1125–1128, 2004. DOI: 10.1126/science.1100700.

[27] F. Meinert, M. Panfil, M. Mark, K. Lauber, J.-S. Caux, and H.-C. Nägerl, "Probing the excitations of a lieb-liniger gas from weak to strong coupling," *Phys. Rev. Lett.*, vol. 115, no. 8, 2015. DOI: 10.1103/physrevlett.115.085301.

[28] G. Boéris *et al.*, "Mott transition for strongly interacting one-dimensional bosons in a shallow periodic potential," *Phys. Rev. A*, vol. 93, p. 011 601, 1 Jan. 2016. DOI: 10.1103/PhysRevA.93.011601.

[29] A. F. Andreev and I. M. Lifshitz, "Quantum Theory of Defects in Crystals," *Soviet Journal of Experimental and Theoretical Physics*, vol. 29, p. 1107, Jan. 1969.

[30] H. Matsuda and T. Tsuneto, "Off-diagonal long-range order in solids," *Progr. Theor. Phys.*, vol. 46, pp. 411–436, 1970. DOI: 10.1143/PTPS.46.411.

[31] K. S. Liu and M. E. Fisher, "Quantum lattice gas and the existence of a supersolid," *J. Low Temp. Phys.*, vol. 10, no. 5, pp. 655–683, 1973.

[32] G. G. Batrouni and R. T. Scalettar, "Phase separation in supersolids," *Phys. Rev. Lett.*, vol. 84, pp. 1599–1602, 7 Feb. 2000. DOI: 10.1103/PhysRevLett.84.1599.

[33] F. Hébert, G. G. Batrouni, R. T. Scalettar, G. Schmid, M. Troyer, and A. Dorneich, "Quantum phase transitions in the two-dimensional hardcore boson model," *Phys. Rev. B*, vol. 65, p. 014 513, 1 Dec. 2001. DOI: 10.1103/PhysRevB.65.014513.

[34] M. Boninsegni, "Phase separation in mixtures of hard core bosons," *Phys. Rev. Lett.*, vol. 87, p. 087 201, 8 Aug. 2001. DOI: 10.1103/PhysRevLett.87.087201.

[35] D. Heidarian and K. Damle, "Persistent supersolid phase of hard-core bosons on the triangular lattice," *Phys. Rev. Lett.*, vol. 95, p. 127 206, 12 Sep. 2005. DOI: 10.1103/PhysRevLett.95.127206.

[36] R. G. Melko, A. Paramekanti, A. A. Burkov, A. Vishwanath, D. N. Sheng, and L. Balents, "Supersolid order from disorder: Hard-core bosons on the triangular lattice," *Phys. Rev. Lett.*, vol. 95, p. 127 207, 12 Sep. 2005. DOI: 10.1103/PhysRevLett.95.127207.

[37] S. Wessel and M. Troyer, "Supersolid hard-core bosons on the triangular lattice," *Phys. Rev. Lett.*, vol. 95, p. 127 205, 12 Sep. 2005. DOI: 10.1103/PhysRevLett.95.127205.

[38] M. Boninsegni and N. Prokof'ev, "Supersolid phase of hard-core bosons on a triangular lattice," *Phys. Rev. Lett.*, vol. 95, p. 237 204, 23 Nov. 2005. DOI: 10.1103/PhysRevLett.95.237204.

[39] P. H. Nguyen and M. Boninsegni, "Phase diagram of hard core bosons with anisotropic interactions," *J. Low Temp. Phys.*, Jul. 2022. DOI: 10.1007/s10909-022-02793-x.

[40] N. Prokof'ev, B. Svistunov, and I. Tupitsyn, ""worm" algorithm in quantum monte carlo simulations," *Phys. Lett. A*, vol. 238, no. 4, pp. 253–257, 1998. DOI: https://doi.org/10.1016/S0375-9601(97)00957-2.

[41] L. Pollet, K. V. Houcke, and S. M. Rombouts, "Engineering local optimality in quantum monte carlo algorithms," *J. Comput. Phys.*, vol. 225, no. 2, pp. 2249–2266, 2007. DOI: https://doi.org/10.1016/j.jcp.2007.03.013.

[42] E. L. Pollock and D. M. Ceperley, "Path-integral computation of superfluid densities," *Physical Review B*, vol. 36, no. 16, p. 8343, 1987. DOI: 10.1103/PhysRevB.36.8343.

[43] J. J. Sakurai and J. Napolitano, *Modern quantum mechanics; 2nd ed.* San Francisco, CA: Addison-Wesley, 2011. [Online]. Available: https://cds.cern.ch/record/1341875.

[44] D. J. Bishop and J. D. Reppy, "Study of the superfluid transition in two-dimensional ^{4}He films," *Phys. Rev. Lett.*, vol. 40, pp. 1727–1730, 26 Jun. 1978. DOI: 10.1103/PhysRevLett.40.1727. [Online]. Available: https://link.aps.org/doi/10.1103/PhysRevLett.40.1727.

[45] G. Agnolet, D. F. McQueeney, and J. D. Reppy, "Kosterlitz-thouless transition in helium films," *Phys. Rev. B*, vol. 39, no. 13, pp. 8934–8958, 1989. DOI: 10.1103/PhysRevB.39.8934.

[46] G. Csáthy, D. Tulimieri, J. Yoon, and M. H. W. Chan, "Heat capacity and superfluid density of thin ^{4}he films on porous gold and on h_2," *Phys. Rev. Lett.*, vol. 80, no. 20, pp. 4482–4485, 1998. DOI: 10.1103/PhysRevLett.80.4482.

[47] M. Boninsegni, M. W. Cole, and F. Toigo, "Helium adsorption on a lithium substrate," *Phys. Rev. Lett.*, vol. 83, pp. 2002–2005, 1999. DOI: 10.1103/PhysRevLett.83.2002.

[48] E. Van Cleve, P. Taborek, and J. M. Rutledge, "Helium adsorption on lithium substrate," *J. Low Temp. Phys.*, vol. 150, pp. 1–11, 2008. DOI: 10.1007/s10909-007-9516-5.

[49] J. M. Kosterlitz, "Superfluidity in thin films of ^{4}he," *J. Low Temp. Phys.*, vol. 201, pp. 504–581, 2020. DOI: 10.1007/s10909-019-02335-y.

[50] B. A. Huberman and J. G. Dash, "Onset of superflow in thin helium films," *Phys. Rev. B*, vol. 17, pp. 398–401, 1 Jan. 1978. DOI: 10.1103/PhysRevB.17.398. [Online]. Available: https://link.aps.org/doi/10.1103/PhysRevB.17.398.

[51] K. K. Mon and W. F. Saam, "Two-layer XY model for ^{4}He films," *Phys. Rev. B*, vol. 22, pp. 3221–3229, 7 Oct. 1980. DOI: 10.1103/PhysRevB.22.3221. [Online]. Available: https://link.aps.org/doi/10.1103/PhysRevB.22.3221.

[52] N. Schultka and E. Manousakis, "Specific heat of superfluids near the transition temperature," *Physical Review B*, vol. 52, no. 10, p. 7528, 1995. DOI: 10.1103/PhysRevB.52.7528.

[53] N. Schultka and E. Manousakis, "Crossover from two- to three-dimensional behavior in superfluids," *Phys. Rev. B*, vol. 51, pp. 11 712–11 720, 17 1995. DOI: 10.1103/PhysRevB.51.11712.

[54] Y. Komura and Y. Okabe, "Large-scale monte carlo simulation of two-dimensional classical xy model using multiple gpus," *Journal of the Physical Society of Japan*, vol. 81, no. 11, p. 113 001, 2012. DOI: 10.1143/JPSJ.81.113001.

[55] J. Tobochnik and G. V. Chester, "Monte carlo study of the planar spin model," *Physical Review B*, vol. 20, no. 9, pp. 3761–3769, 1979. DOI: 10.1103/PhysRevB.20.3761.

[56] H. G. Evertz and D. P. Landau, "Critical dynamics in the two-dimensional classical xy model: A spin-dynamics study," *Phys. Rev. B*, vol. 54, pp. 12 302–12 317, 17 Nov. 1996. DOI: 10.1103/PhysRevB.54.12302. [Online]. Available: https://link.aps.org/doi/10.1103/PhysRevB.54.12302.

[57] A. Cuccoli, V. Tognetti, and R. Vaia, "Two-dimensional xxz model on a square lattice: A monte carlo simulation," *Phys. Rev. B*, vol. 52, pp. 10 221–10 231, 14 Oct. 1995. DOI: 10.1103/PhysRevB.52.10221. [Online]. Available: https://link.aps.org/doi/10.1103/PhysRevB.52.10221.

[58] M. Hasenbusch, "The two-dimensional xy model at the transition temperature: A high-precision monte carlo study," *Journal of Physics A: Mathematical and General*, vol. 38, pp. 5869–5884, 2005. DOI: 10.1088/0305-4470/38/26/003.

[59] Y.-D. Hsieh, Y.-J. Kao, and A. W. Sandvik, "Finite-size scaling method for the berezinskii–kosterlitz–thouless transition," *Journal of Statistical Mechanics: Theory and Experiment*, vol. 2013, P09001, 2013. DOI: 10.1088/1742-5468/2013/09/P09001.

[60] B.-Z. Wang, P. Hou, C.-J. Huang, and Y. Deng, "Percolation of the two-dimensional XY model in the flow representation," *Phys. Rev. E*, vol. 103, p. 062 131, 6 Jun. 2021. DOI: 10.1103/PhysRevE.103.062131. [Online]. Available: https://link.aps.org/doi/10.1103/PhysRevE.103.062131.

[61] L. M. Steele, C. J. Yeager, and D. Finotello, "Precision specific-heat studies of thin superfluid films," *Phys. Rev. Lett.*, vol. 71, pp. 3673–3676, 22 Nov. 1993. DOI: 10.1103/PhysRevLett.71.3673. [Online]. Available: https://link.aps.org/doi/10.1103/PhysRevLett.71.3673.

[62] M. Boninsegni and S. Moroni, "Specific heat of thin ^{4}He films on graphite," *Phys. Rev. B*, vol. 102, p. 235 436, 23 Dec. 2020. DOI: 10.1103/PhysRevB.102.235436. [Online]. Available: https://link.aps.org/doi/10.1103/PhysRevB.102.235436.

[63] D. R. Nelson and J. M. Kosterlitz, "Universal jump in the superfluid density of two-dimensional superfluids," *Physical Review Letters*, vol. 39, no. 19, p. 1201, 1977. DOI: 10.1103/PhysRevLett.39.1201.

[64] N. V. Prokof'ev and B. V. Svistunov, "Two definitions of superfluid density," *Phys. Rev. B*, vol. 61, pp. 11 282–11 284, 17 May 2000. DOI: 10.1103/PhysRevB.61.11282. [Online]. Available: https://link.aps.org/doi/10.1103/PhysRevB.61.11282.

[65] Y. Tomita and Y. Okabe, "Probability-changing cluster algorithm for two-dimensional xy and clock models," *Physical Review B*, vol. 65, no. 18, p. 184 405, 2002. DOI: 10.1103/PhysRevB.65.184405.

[66] W. Janke and K. Nather, "High-precision monte carlo study of the two-dimensional xy villain model," *Physical Review B*, vol. 48, no. 10, p. 7419, 1993. DOI: 10.1103/PhysRevB.48.7419.

[67] H. Gould, J. Tobochnik, and C. Wolfgang, *An Introduction to Computer Simulation Methods: Applications to Physical Systems (3rd Edition)*. San Francisco, USA: Addison-Wesley Longman Publishing Co., Inc., 2006, ISBN: 0805377581. DOI: 10.1119/1.2219401.

[68] P. Jakubczyk and A. Eberlein, "Thermodynamics of the two-dimensional XY model from functional renormalization," *Phys. Rev. E*, vol. 93, p. 062 145, 6 Jun. 2016. DOI: 10.1103/PhysRevE.93.062145. [Online]. Available: https://link.aps.org/doi/10.1103/PhysRevE.93.062145.

[69] S. Ota, S. B. Ota, and M. Fahnle, "Microcanonical monte carlo simulations for the two-dimensional xy model," *Journal of Physics: Condensed Matter*, vol. 4, no. 24, p. 5411, 1992. DOI: 10.1088/0953-8984/4/24/011.

[70] S. Ota and S. Ota, "Vortices in the 2d classical *xy*-model: A microcanonical monte-carlo simulation study," English, *Phys. Lett. A*, vol. 206, no. 1-2, 133–136, Oct. 1995, ISSN: 0375-9601. DOI: {10.1016/0375-9601(95)00588-T}.

[71] D. Giuliano, P. H. Nguyen, A. Nava, and M. Boninsegni, "Uniaxial modulation and the berezinskii-kosterlitz-thouless transition," 2023. DOI: 10.48550/ARXIV.2302.10335. [Online]. Available: https://arxiv.org/abs/2302.10335.

[72] Y. Kora, M. Boninsegni, D. T. Son, and S. Zhang, "Tuning the quantumness of simple bose systems: A universal phase diagram," *Proc. Natl. Acad. Sci.*, vol. 117, no. 44, pp. 27 231–27 237, 2020. DOI: 10.1073/pnas.2017646117.

[73] J. V. José, L. P. Kadanoff, S. Kirkpatrick, and D. R. Nelson, "Renormalization, vortices, and symmetry-breaking perturbations in the two-dimensional planar model," *Phys. Rev. B*, vol. 16, pp. 1217–1241, 3 Aug. 1977. DOI: 10.1103/PhysRevB.16.1217.

[74] T. Ohta and D. Jasnow, "XY Model and the superfluid density in two dimensions," *Phys. Rev. B*, vol. 20, pp. 139–146, 1 Jul. 1979. DOI: 10.1103/PhysRevB.20.139.

[75] A. Del Maestro and I. Affleck, "Interacting bosons in one dimension and the applicability of luttinger-liquid theory as revealed by path-integral quantum monte carlo calculations," *Phys. Rev. B*, vol. 82, p. 060 515, 6 Aug. 2010. DOI: 10.1103/PhysRevB.82.060515. [Online]. Available: https://link.aps.org/doi/10.1103/PhysRevB.82.060515.

[76] A. Del Maestro, M. Boninsegni, and I. Affleck, "^{4}He Luttinger liquid in nanopores," *Phys. Rev. Lett.*, vol. 106, p. 105 303, 10 Mar. 2011. DOI: 10.1103/PhysRevLett.106.105303. [Online]. Available: https://link.aps.org/doi/10.1103/PhysRevLett.106.105303.

[77] W. A. Little, "Decay of persistent currents in small superconductors," *Phys. Rev.*, vol. 156, pp. 396–403, 2 Apr. 1967. DOI: 10.1103/PhysRev.156.396.

[78] D. E. McCumber and B. I. Halperin, "Time scale of intrinsic resistive fluctuations in thin superconducting wires," *Phys. Rev. B*, vol. 1, pp. 1054–1070, 3 Feb. 1970. DOI: 10.1103/PhysRevB.1.1054.

[79] A. D. Zaikin, D. S. Golubev, A. van Otterlo, and G. T. Zimányi, "Quantum phase slips and transport in ultrathin superconducting wires," *Phys. Rev. Lett.*, vol. 78, pp. 1552–1555, 8 Feb. 1997. DOI: 10.1103/PhysRevLett.78.1552.

[80] J. A. Freire, D. P. Arovas, and H. Levine, "Quantum nucleation of phase slips in a $1D$ model of a superfluid," *Phys. Rev. Lett.*, vol. 79, pp. 5054–5057, 25 Dec. 1997. DOI: 10.1103/PhysRevLett.79.5054.

[81] Y. Kagan, N. V. Prokof'ev, and B. V. Svistunov, "Supercurrent stability in a quasi-one-dimensional weakly interacting bose gas," *Phys. Rev. A*, vol. 61, p. 045 601, 4 Mar. 2000. DOI: 10.1103/PhysRevA.61.045601.

[82] S. I. Shevchenko, *Sov. J. Low Temp. Phys.*, no. 14, p. 553, 1988.

[83] M. Boninsegni, A. B. Kuklov, L. Pollet, N. V. Prokof'ev, B. V. Svistunov, and M. Troyer, "Luttinger liquid in the core of a screw dislocation in helium-4," *Phys. Rev. Lett.*, vol. 99, p. 035 301, 3 Jul. 2007. DOI: 10.1103/PhysRevLett.99.035301.

[84] E. Van Cleve, P. Taborek, and J. E. Rutledge, "Helium adsorption on a lithium substrate," *J. Low Temp. Phys.*, vol. 150, pp. 1–11, 2008. DOI: 10.1007/s10909-007-9516-5.

[85] K. Epstein, A. M. Goldman, and A. M. Kadin, "Vortex-antivortex pair dissociation in two-dimensional superconductors," *Phys. Rev. Lett.*, vol. 47, pp. 534–537, 7 Aug. 1981. DOI: 10.1103/PhysRevLett.47.534. [Online]. Available: https://link.aps.org/doi/10.1103/PhysRevLett.47.534.

[86] D. J. Resnick, J. C. Garland, J. T. Boyd, S. Shoemaker, and R. S. Newrock, "Kosterlitz-thouless transition in proximity-coupled superconducting arrays," *Phys. Rev. Lett.*, vol. 47, pp. 1542–1545, 21 Nov. 1981. DOI: 10.1103/PhysRevLett.47.1542. [Online]. Available: https://link.aps.org/doi/10.1103/PhysRevLett.47.1542.

[87] Z. Hadzibabic, P. Krüger, M. Cheneau, B. Battelier, and J. Dalibard, "Berezinskii-kosterlitz-thouless crossover in a trapped atomic gas," *Nature*, vol. 441, pp. 1118–1121, 2006. DOI: 110.1038/nature04851. [Online]. Available: https://doi.org/10.1038/nature04851.

[88] R. Desbuquois *et al.*, "Superfluid behaviour of a two-dimensional bose gas," *Nat. Phys.*, vol. 8, pp. 645–648, 2012. DOI: 10.1038/nphys2378.

[89] R. J. Fletcher *et al.*, "Connecting berezinskii-kosterlitz-thouless and bec phase transitions by tuning interactions in a trapped gas," *Phys. Rev. Lett.*, vol. 114, p. 255 302, 25 Jun. 2015. DOI: 10.1103/PhysRevLett.114.255302.

[90] S. Sunami *et al.*, "Observation of the berezinskii-kosterlitz-thouless transition in a two-dimensional bose gas via matter-wave interferometry," *Phys. Rev. Lett.*, vol. 128, p. 250 402, 25 Jun. 2022. DOI: 10.1103/PhysRevLett.128.250402. [Online]. Available: https://link.aps.org/doi/10.1103/PhysRevLett.128.250402.

[91] P. E. Sokol, M. R. Gibbs, W. G. Stirling, R. T. Azuah, and M. A. Adams, "Microscopic origins of superfluidity in confined geometries," *Nature (London)*, vol. 379, pp. 616–618, 1996. DOI: 10.1038/379616a0.

[92] R. M. Dimeo, P. E. Sokol, C. R. Anderson, W. G. Stirling, K. H. Andersen, and M. A. Adams, "Localized collective excitations in superfluid helium in vycor," *Phys. Rev. Lett.*, vol. 81, pp. 5860–5863, 26 Dec. 1998. DOI: 10.1103/PhysRevLett.81.5860.

[93] O. Plantevin *et al.*, "Excitations of superfluid ^{4}He in porous media: Aerogel and vycor," *Phys. Rev. B*, vol. 63, p. 224 508, 22 May 2001. DOI: 10.1103/PhysRevB.63.224508.

[94] C. R. Anderson, K. H. Andersen, W. G. Stirling, P. E. Sokol, and R. M. Dimeo, "Dynamics of superfluid ^{4}He confined in xerogel glass," *Phys. Rev. B*, vol. 65, p. 174 509, 17 Apr. 2002. DOI: 10.1103/PhysRevB.65.174509.

[95] R. Toda *et al.*, "Superfluidity of ^{4}He in one and three dimensions realized in nanopores," *Phys. Rev. Lett.*, vol. 99, p. 255 301, 25 Dec. 2007. DOI: 10.1103/PhysRevLett.99.255301.

[96] T. R. Prisk *et al.*, "Phases of superfluid helium in smooth cylindrical pores," *Phys. Rev. B*, vol. 88, p. 014 521, 1 Jul. 2013. DOI: 10.1103/PhysRevB.88.014521.

[97] M. Savard, G. Dauphinais, and G. Gervais, "Hydrodynamics of superfluid helium in a single nanohole," *Phys. Rev. Lett.*, vol. 107, p. 254 501, 25 Dec. 2011. DOI: 10.1103/PhysRevLett.107.254501.

[98] W. Teizer, R. B. Hallock, E. Dujardin, and T. W. Ebbesen, "^4He Desorption from single wall carbon nanotube bundles: A one-dimensional adsorbate," *Phys. Rev. Lett.*, vol. 82, pp. 5305–5308, 26 Jun. 1999. DOI: 10.1103/PhysRevLett.82.5305.

[99] T. Ohba, "Limited quantum helium transportation through nano-channels by quantum fluctuation," *Sci. Rep.*, vol. 6, p. 28 992, 16 2016. DOI: 10.1038/srep28992.

[100] M. Wenzel, F. Böttcher, T. Langen, I. Ferrier-Barbut, and T. Pfau, "Striped states in a many-body system of tilted dipoles," *Phys. Rev. A*, vol. 96, p. 053 630, 5 Nov. 2017. DOI: 10.1103/PhysRevA.96.053630.

[101] G. Biagioni *et al.*, "Dimensional crossover in the superfluid-supersolid quantum phase transition," *Phys. Rev. X*, vol. 12, p. 021 019, 2 Apr. 2022. DOI: 10.1103/PhysRevX.12.021019.

[102] M. Boninsegni, "Supersolid phases of cold atom assemblies," *J. Low Temp. Phys.*, vol. 168, no. 3-4, pp. 137–149, 2012. DOI: 10.1007/s10909-012-0571-1.

[103] Y. Kora and M. Boninsegni, "Patterned supersolids in dipolar bose systems," *J. Low Temp. Phys.*, vol. 197, no. 5-6, pp. 337–347, 2019. DOI: 10.1007/s10909-019-02229-z.

[104] H. Moraal, "Statistical mechanics of quasi-one-dimensional systems," *Physica A*, vol. 85, no. 3, pp. 457–484, 1976, ISSN: 0378-4371. [Online]. Available: https://www.sciencedirect.com/science/article/pii/0378437176900200.

[105] M. W. Cole *et al.*, "Condensation of helium in nanotube bundles," *Phys. Rev. Lett.*, vol. 84, pp. 3883–3886, 17 Apr. 2000. DOI: 10.1103/PhysRevLett.84.3883.

[106] M. Boninsegni, S.-Y. Lee, and V. H. Crespi, "Helium in one-dimensional nanopores: Free dispersion, localization, and commensurate/incommensurate transitions with nonrigid orbitals," *Phys. Rev. Lett.*, vol. 86, pp. 3360–3363, 15 Apr. 2001. DOI: 10.1103/PhysRevLett.86.3360. [Online]. Available: https://link.aps.org/doi/10.1103/PhysRevLett.86.3360.

[107] P. Kalinay, "Effective transport equations in quasi 1d systems," *The European Physical Journal Special Topics*, vol. 223, no. 14, pp. 3027–3043, Dec. 2014, ISSN: 1951-6401. DOI: 10.1140/epjst/e2014-02317-5.

[108] B. Béri and N. R. Cooper, "Topological kondo effect with majorana fermions," *Phys. Rev. Lett.*, vol. 109, p. 156 803, 15 Oct. 2012. DOI: 10.1103/PhysRevLett.109.156803. [Online]. Available: https://link.aps.org/doi/10.1103/PhysRevLett.109.156803.

[109] B. Béri, "Majorana-klein hybridization in topological superconductor junctions," *Phys. Rev. Lett.*, vol. 110, p. 216 803, 21 May 2013. DOI: 10.1103/PhysRevLett.110.216803. [Online]. Available: https://link.aps.org/doi/10.1103/PhysRevLett.110.216803.

[110] A. Altland and R. Egger, "Multiterminal coulomb-majorana junction," *Phys. Rev. Lett.*, vol. 110, p. 196 401, 19 May 2013. DOI: 10.1103/PhysRevLett.110.196401. [Online]. Available: https://link.aps.org/doi/10.1103/PhysRevLett.110.196401.

[111] D. Giuliano, L. Lepori, and A. Nava, "Tunable spin/charge kondo effect at a double superconducting island connected to two spinless quantum wires," *Phys. Rev. B*, vol. 101, p. 195 140, 19 May 2020. DOI: 10.1103/PhysRevB.101.195140. [Online]. Available: https://link.aps.org/doi/10.1103/PhysRevB.101.195140.

[112] D. Giuliano, A. Nava, R. Egger, P. Sodano, and F. Buccheri, "Multiparticle scattering and breakdown of the Wiedemann-Franz law at a junction of N interacting quantum wires," *Phys. Rev. B*, vol. 105, p. 035 419, 3 Jan. 2022. DOI: 10.1103/PhysRevB.105.035419. [Online]. Available: https://link.aps.org/doi/10.1103/PhysRevB.105.035419.

[113] D. Giuliano, A. Nava, and P. Sodano, "Tunable kondo screening length at a Y-junction of three inhomogeneous spin chains," *Nucl. Phys. B*, vol. 960, p. 115 192, 2020, ISSN: 0550-3213. DOI: https://doi.org/10.1016/j.nuclphysb.2020.115192. [Online]. Available: https://www.sciencedirect.com/science/article/pii/S0550321320302777.

[114] F. Buccheri, A. Nava, R. Egger, P. Sodano, and D. Giuliano, "Violation of the Wiedemann-Franz law in the topological kondo model," *Phys. Rev. B*, vol. 105, p. L081403, 8 Feb. 2022. DOI: 10.1103/PhysRevB.105.L081403. [Online]. Available: https://link.aps.org/doi/10.1103/PhysRevB.105.L081403.

[115] M. Wallin, E. S. So/rensen, S. M. Girvin, and A. P. Young, "Superconductor-insulator transition in two-dimensional dirty boson systems," *Phys. Rev. B*, vol. 49, pp. 12 115–12 139, 17 May 1994. DOI: 10.1103/PhysRevB.49.12115. [Online]. Available: https://link.aps.org/doi/10.1103/PhysRevB.49.12115.

[116] K. Yamashita and D. S. Hirashima, "Superfluid density of ^{4}He confined in nanopores," *Phys. Rev. B*, vol. 79, p. 014 501, 1 Jan. 2009. DOI: 10.1103/PhysRevB.79.014501. [Online]. Available: https://link.aps.org/doi/10.1103/PhysRevB.79.014501.

[117] W. Yang and I. Affleck, "Shell model for superfluids in rough-walled nanopores," *Phys. Rev. B*, vol. 102, p. 205 426, 20 Nov. 2020. DOI: 10.1103/PhysRevB.102.205426.

[118] A. Nava, D. Giuliano, P. H. Nguyen, and M. Boninsegni, "Quasi-one-dimensional ^{4}He in nanopores," *Phys. Rev. B*, vol. 105, p. 085 402, 8 Feb. 2022. DOI: 10.1103/PhysRevB.105.085402.

[119] C. Chamon, M. Oshikawa, and I. Affleck, "Junctions of three quantum wires and the dissipative hofstadter model," *Phys. Rev. Lett.*, vol. 91, p. 206 403, 20 Nov. 2003. DOI: 10.1103/PhysRevLett.91.206403. [Online]. Available: https://link.aps.org/doi/10.1103/PhysRevLett.91.206403.

[120] M. Oshikawa, C. Chamon, and I. Affleck, "Junctions of three quantum wires," *Journal of Statistical Mechanics: Theory and Experiment*, vol. 2006, no. 02, P02008, Feb. 2006, ISSN: 1742-5468. DOI: 10.1088/1742-5468/2006/02/p02008. [Online]. Available: http://dx.doi.org/10.1088/1742-5468/2006/02/P02008.

[121] C.-Y. Hou, A. Rahmani, A. E. Feiguin, and C. Chamon, "Junctions of multiple quantum wires with different luttinger parameters," *Phys. Rev. B*, vol. 86, p. 075 451, 7 Aug. 2012. DOI: 10.1103/PhysRevB.86.075451. [Online]. Available: https://link.aps.org/doi/10.1103/PhysRevB.86.075451.

[122] D. Giuliano and P. Sodano, "Boundary field theory approach to the renormalization of squid devices," *Nuclear Physics B*, vol. 770, no. 3, pp. 332–370, 2007, ISSN: 0550-3213. DOI: https://doi.org/10.1016/j.nuclphysb.2007.02.015. [Online]. Available: https://www.sciencedirect.com/science/article/pii/S0550321307001484.

[123] D. Giuliano and I. Affleck, "Real fermion modes, impurity entropy, and nontrivial fixed points in the phase diagram of junctions of interacting quantum wires and topological superconductors," *Nuclear Physics B*, vol. 944, p. 114 645, 2019, ISSN: 0550-3213. DOI: https://doi.org/10.1016/j.nuclphysb.2019.114645. [Online]. Available: https://www.sciencedirect.com/science/article/pii/S0550321319301312.

[124] C. L. Kane, D. Giuliano, and I. Affleck, "Equivalent critical behavior of a helical point contact and a two-channel luttinger liquid–topological superconductor junction," *Phys. Rev. Research*, vol. 2, p. 023 243, 2 May 2020. DOI: 10.1103/PhysRevResearch.2.023243. [Online]. Available: https://link.aps.org/doi/10.1103/PhysRevResearch.2.023243.

[125] J. Medina, D. Green, and C. Chamon, "Networks of quantum wire junctions: A system with quantized integer hall resistance without vanishing longitudinal resistivity," *Phys. Rev. B*, vol. 87, p. 045 128, 4 Jan. 2013. DOI: 10.1103/PhysRevB.87.045128. [Online]. Available: https://link.aps.org/doi/10.1103/PhysRevB.87.045128.

[126] E. Novais, A. H. Castro Neto, L. Borda, I. Affleck, and G. Zarand, "Frustration of decoherence in open quantum systems," *Phys. Rev. B*, vol. 72, p. 014 417, 1 Jul. 2005. DOI: 10.1103/PhysRevB.72.014417.

[127] D. Giuliano and P. Sodano, "Frustration of decoherence in y-shaped superconducting josephson networks," *New Journal of Physics*, vol. 10, no. 9, p. 093 023, Sep. 2008. DOI: 10.1088/1367-2630/10/9/093023.

[128] D. Jaksch, C. Bruder, J. I. Cirac, C. W. Gardiner, and P. Zoller, "Cold bosonic atoms in optical lattices," *Phys. Rev. Lett.*, vol. 81, pp. 3108–3111, 15 Oct. 1998. DOI: 10.1103/PhysRevLett.81.3108.

[129] R. Grimm, M. Weidemüller, and Y. B. Ovchinnikov, "Optical dipole traps for neutral atoms," in ser. Advances In Atomic, Molecular, and Optical Physics, B. Bederson and H. Walther, Eds., vol. 42, Academic Press, 2000, pp. 95–170. DOI: 10.1016/S1049-250X(08)60186-X.

[130] M. Lewenstein, A. Sanpera, V. Ahufinger, B. Damski, A. Sen De, and U. Sen, "Ultracold atomic gases in optical lattices: Mimicking condensed matter physics and beyond," *Advances in Physics*, vol. 56, no. 2, pp. 243–379, 2007. DOI: 10.1080/00018730701223200.

[131] P. Windpassinger and K. Sengstock, "Engineering novel optical lattices," *Rep. Progr. Phys.*, vol. 76, no. 8, p. 086 401, Jul. 2013. DOI: 10.1088/0034-4885/76/8/086401.

[132] O. Dutta *et al.*, "Non-standard hubbard models in optical lattices: A review," *Rep. Progr. Phys.*, vol. 78, no. 6, p. 066 001, May 2015. DOI: 10.1088/0034-4885/78/6/066001.

[133] C. J. Pethick and H. Smith, *Bose–Einstein Condensation in Dilute Gases*. Cambridge University Press, 2008.

[134] N. Henkel, R. Nath, and T. Pohl, "Three-dimensional roton excitations and supersolid formation in rydberg-excited bose-einstein condensates," *Phys. Rev. Lett.*, vol. 104, p. 195 302, 19 May 2010. DOI: 10.1103/PhysRevLett.104.195302.

[135] B. Juliá-Díaz, T. Graß, O. Dutta, D. E. Chang, and M. Lewenstein, "Engineering p-wave interactions in ultracold atoms using nanoplasmonic traps," *Nat. Comm.*, vol. 4, p. 2046, 1 2013. DOI: 10.1038/ncomms3046.

[136] S.-P. Yu, J. A. Muniz, C.-L. Hung, and H. J. Kimble, "Two-dimensional photonic crystals for engineering atom–light interactions," *Proc. Natl. Acad, Sci.*, vol. 116, no. 26, pp. 12 743–12 751, 2019. DOI: 10.1073/pnas.1822110116.

[137] T Xie *et al.*, "Engineering long-range interactions between ultracold atoms with light," *J. Phys. B: At., Mol. Opt. Phys.*, vol. 55, no. 3, p. 034 001, Feb. 2022. DOI: 10.1088/1361-6455/ac4b40.

[138] C. Schweizer *et al.*, "Floquet approach to 2 lattice gauge theories with ultracold atoms in optical lattices," *Nat. Phys.*, vol. 15, no. 11, pp. 1168–1173, 2019, ISSN: 1745-2473. DOI: 10.1038/s41567-019-0649-7.

[139] M. Aidelsburger *et al.*, "Cold atoms meet lattice gauge theory," *Phil. Trans. Royal Soc. A: Math. Phys. Eng. Sci.*, vol. 380, no. 2216, 2022. DOI: 10.1098/rsta.2021.0064.

[140] E. A. L. Henn, J. Billy, and T. Pfau, "Dipolar gases – experiments," in *Quantum Gas Experiments*, ser. Cold Atoms, P. Törmä and K. Sengstock, Eds., vol. 3, World Scientific Publishing, 2014, pp. 311–325. DOI: 10.1142/9781783264766_0014.

[141] M. Baranov, "Theoretical progress in many-body physics with ultracold dipolar gases," *Phys. Rep.*, vol. 464, no. 3, pp. 71–111, 2008. DOI: https://doi.org/10.1016/j.physrep.2008.04.007.

[142] T Lahaye, C Menotti, L Santos, M Lewenstein, and T Pfau, "The physics of dipolar bosonic quantum gases," *Rep. Prog. Phys.*, vol. 72, no. 12, p. 126 401, Nov. 2009. DOI: 10.1088/0034-4885/72/12/126401.

[143] F. Cinti and M. Boninsegni, "Classical and quantum filaments in the ground state of trapped dipolar bose gases," *Phys. Rev. A*, vol. 96, p. 013 627, 1 Jul. 2017. DOI: 10.1103/PhysRevA.96.013627.

[144] B. Spivak and S. A. Kivelson, "Phases intermediate between a two-dimensional electron liquid and wigner crystal," *Phys. Rev. B*, vol. 70, p. 155 114, 15 Oct. 2004. DOI: 10.1103/PhysRevB.70.155114.

[145] S. Moroni and M. Boninsegni, "Coexistence, interfacial energy, and the fate of microemulsions of 2d dipolar bosons," *Phys. Rev. Lett.*, vol. 113, p. 240 407, 24 Dec. 2014. DOI: 10.1103/PhysRevLett.113.240407.

[146] L. Pollet, J. D. Picon, H. P. Büchler, and M. Troyer, "Supersolid phase with cold polar molecules on a triangular lattice," *Phys. Rev. Lett.*, vol. 104, no. 12, pp. 125 302–125 302, 2010. DOI: 10.1103/PhysRevLett.104.125302.

[147] C. Zhang, A. Safavi-Naini, A. M. Rey, and B. Capogrosso-Sansone, "Equilibrium phases of tilted dipolar lattice bosons," *New J. Phys.*, vol. 17, p. 9, 2015, ISSN: 1367-2630. DOI: 10.1088/1367-2630/17/12/123014.

[148] F. Cinti and M. Boninsegni, "Absence of superfluidity in 2d dipolar bose striped crystals," *J. Low Temp. Phys.*, vol. 196, no. 5-6, pp. 413–422, 2019. DOI: 10.1007/s10909-019-02209-3.

[149] Y. C. Chen, R. G. Melko, S. Wessel, and Y. J. Kao, "Supersolidity from defect condensation in the extended boson hubbard model," *Phys. Rev. B*, vol. 77, no. 1, p. 014 524, 2008. DOI: 10.1103/PhysRevB.77.014524.

[150] L. Dang, M. Boninsegni, and L. Pollet, "Vacancy supersolid of hard-core bosons on the square lattice," *Phys. Rev. B*, vol. 78, p. 132 512, 13 Oct. 2008. DOI: 10.1103/PhysRevB.78.132512.

[151] N. Prokof'ev and B. Svistunov, "Supersolid state of matter," *Phys. Rev. Lett.*, vol. 94, no. 15, pp. 155 302–155 302, 2005. DOI: 10.1103/PhysRevLett.94.155302.

[152] L. Dang, M. Boninsegni, and L. Pollet, "Disorder-induced superfluidity," *Phys. Rev. B*, vol. 79, no. 21, pp. 214 529–214 529, 2009. DOI: 10.1103/PhysRevB.79.214529.

[153] E. L. Pollock and D. M. Ceperley, "Path-integral computation of superfluid densities," *Phys. Rev. B*, vol. 36, no. 16, pp. 8343–8352, 1987.

[154] H.-K. Wu and W.-L. Tu, "Competing quantum phases of hard-core bosons with tilted dipole-dipole interaction," *Phys. Rev. A*, vol. 102, p. 053 306, 5 Nov. 2020. DOI: 10.1103/PhysRevA.102.053306. [Online]. Available: https://link.aps.org/doi/10.1103/PhysRevA.102.053306.